Quantifying distribution of above ground biomass estimates in forested areas across LiDAR applications and multiple scales

by

Srishanth Srikumar

A thesis
presented to the University of Waterloo
in fulfillment of the
thesis requirement for the degree of
Master of Science
in
Geography

Waterloo, Ontario, Canada, 2025

© Srishanth Srikumar 2025

Author's Declaration

I hereby declare that I am the sole author of this thesis. This is a true copy of the thesis, including any required final revisions, as accepted by my examiners.

I understand that my thesis may be made electronically available to the public.

Abstract

Accurate quantification of forest biomass is essential for understanding carbon dynamics, preserving biodiversity, and advancing Nature-based Solutions (NbS) in Canada (Seddon et al., 2020). NbS harness, protect, or restore natural ecosystems to address complex environmental challenges. This thesis leverages LiDAR-derived point cloud data to estimate above-ground biomass (AGB), acknowledging that accuracy varies among different LiDAR sensors due to limitations like point density and survey altitude. We evaluated the effectiveness of three remote sensing technologies—Remotely Piloted Aircraft (RPA) LiDAR, aerial LiDAR, and Global Ecosystem Dynamics Investigation (GEDI) satellite LiDAR in estimating AGB across two distinct forested properties, Ballyduff Trails and Christie Bentham Wetland Trails. These remote sensing estimates were compared with traditional in-situ measurements to assess their accuracy and reliability.

Using statistical models and data processing algorithms, we derived AGB estimates from the LiDAR data. Results indicated that both RPA and Aerial LiDAR provided extensive spatial coverage but tended to underestimate AGB compared to in-situ measurements, likely due to the omission of smaller and understory trees. Aerial LiDAR measured higher average tree heights, effectively capturing upper canopy structures, while RPA LiDAR's higher point density facilitated detailed ground-level analysis. Despite its lower spatial resolution, GEDI satellite LiDAR offered a balance between coverage and accuracy, with estimates aligning closely with in-situ values for larger-scale assessments.

This study makes a novel contribution by being among the first to compare these three LiDAR technologies across different forest types in Canada. The findings have significant implications for improving forest management practices, informing conservation strategies, and enhancing carbon accounting methods. By highlighting the strengths and limitations of each remote sensing method, we provide valuable insights for their application in sustainable forest management and climate change mitigation initiatives.

Acknowledgements

I would like to take this opportunity to acknowledge the individuals who have supported and contributed to the completion of this thesis. Their guidance, assistance, and encouragement have been invaluable throughout this journey.

First and foremost, I express my deepest gratitude to my supervisor, Dr. Derek Robinson, for his unwavering support and mentorship during my master's studies. His expertise, insightful feedback, and constant encouragement have been instrumental in shaping this research.

I am also sincerely thankful to Sean Rudd and the entire team at Korotu Technology for sharing their knowledge and assisting with data collection. Their generous contributions and willingness to teach me were crucial in obtaining the data necessary for this study.

A special thanks goes to my partner, Shaieree Cottar, for always being there for me and pushing me to be my best. Your constant support, understanding, and motivation have been a source of strength throughout this process.

Finally, I extend my appreciation to everyone who has supported me along the way. Your encouragement has made this achievement possible, and I am truly grateful for your contributions.

Table of Contents

LIST OF FIGURES ..... **VI**

LIST OF TABLES ..... **VII**

LIST OF ABBREVIATIONS ..... **VIII**

POSITIONALITY STATEMENT ..... **XI**

FIRST CHAPTER – A PRIMER ON LIDAR **1**

1.1 LiDAR Background *1*

1.2 The Role of LiDAR in Forest Management *2*

CHAPTER 2 ..... **7**

1 INTRODUCTION 7

2 METHODS 10

2.1 Study Area *10*

2.2 Data *15*

2.2.1 Data Processing 15

2.2.2 In-situ Data Collection 16

2.2.3 Remotely Piloted Aircraft Data Collection 18

2.2.3 Aerial LiDAR 20

2.2.4 Satellite LiDAR 21

2.3 Analysis *21*

2.3.1 Plot Level Analysis 22

2.3.2 Property-Parcel Level Analysis 23

3 RESULTS 25

3.1 Plot-level analysis *25*

3.2 Property-Parcel analysis *28*

4 DISCUSSION 30

4.1 Limitations *31*

4.2 Other sensors for biomass estimation *32*

5 CONCLUSIONS 34

THIRD CHAPTER: ADVANCEMENTS AND FUTURE CONSIDERATIONS **36**

REFERENCES **42**

APPENDIX A **53**

APPENDIX A (CONTINUED) **54**

APPENDIX A (CONTINUED) **55**

List of Figures

2.1a A detailed view of the Ballyduff Trails study area, highlighting the in-situ plots, GEDI shots, UAV LiDAR scan area, and Aerial LiDAR scan area. The outlined property boundary is also visible within the broader forest landscape……13

2.1b An inset map showing the location of the Ballyduff Trails study area within Ontario, offering a regional context for the research site……..…….……..13

2.2a A detailed view of the Christie Bentham Wetland Trails study area, highlighting the in-situ
plots, GEDI shots, UAV LiDAR scan area, and Aerial LiDAR scan area. The outlined property boundary is also visible within the broader forest landscape……..……14

2.2b An inset map showing the location of the Christie Bentham Wetland Trails study area within Ontario, offering a regional context for the research site……..…….14

2.4 Timeline illustrating the collection of remote sensing and in-situ data at the Ballyduff Trails and Christie Bentham Wetland Trails study sites……16

2.5 Schematic of in-situ data collection……...17

2.6 Plan view of RPA optical and LiDAR scans over Ballyduff and Christie Bentham Wetland Trails showing an RGB visualization of collected point count data, alongside flight lines and digital surface models……..……..……..….19

2.7 Example R code using the lidR package to locate individual treetops within a LiDAR point cloud and calculate tree height metrics…….20

2.9 Interpolated views of in-situ and GEDI over Ballyduff Trails and Christie Bentham Wetland Trails……24

3.1 Box plots represent the distribution of biomass density measurements obtained through four different methods: In-situ, RPA, Aerial, and GEDI……27

List of Tables

3.1 Summary of in-situ plot level characteristics, stem counts, and biomass estimates as well as stem and biomass estimates from other data collection approaches (RPA, Aerial LiDAR, and GEDI).……...26

3.2 Comparison of parcel area, tree density, height, LiDAR point density, and aboveground biomass (AGB) estimates across In-situ, RPA, Aerial, and GEDI methods for Ballyduff and Christie Bentham study sites.…….....29

List of Abbreviations

3D - Three-Dimensional

AGB - Aboveground Biomass

AGL - Above Ground Level

AMCW - Amplitude Modulated Continuous Waveform

ATLAS - Advanced Topographic Laser Altimeter System

BA – Basal Area

BGB - Below Ground Biomass

BT - Ballyduff Trails

c – Speed of Light

C - Carbon

CB - Christie Bentham

DEDSFMP - Digital Elevation Data to Support Flood Mapping

DBH - Diameter at Breast Height

FHIMP - Flood Hazard Identification and Mapping Program

FOV - Field of View

GCP - Ground Control Points

GEDI - Global Ecosystem Dynamic Investigation

GNSS - Global Navigation Satellite System

GPS - Global Positioning System

ICESat-2 - The Ice, Cloud, and Land Elevation Satellite-2

IDW - Inverse Distance Weight

IMU - Inertial Measurement Unit

I**PCC** - Intergovernmental Panel on Climate Change

ISS - International Space Station

KLT - Kawartha Land Trust

LASER - Light Amplification by Stimulated Emission of Radiation

LiDAR - Light Detection and Ranging

L2A - Level 2 A

L2B - Level 2 B

L4A - Level 4 A

L4B - Level 4 B

LULUC - Land Use and Land Use Change

maPoBA - Mid-altitude Piloted-on-Board Aircraft

N/A - Not Applicable

NASA - National Aeronautics and Space Administration

NbS - Nature-based Solutions

NDVI - Normalized Difference Vegetation Index

NIR – Near Infrared

NRCAN - Natural Resource Canada

OMAFRA - Ontario Ministry of Food, Agriculture and Rural Affairs

SFM – Structure from Motion

OSM - OpenStreetMap

PFT - Plant Function Types

PPSM - Points per Square Meter

QGIS - Quantum Geographic Information System

RADAR - Radio Detection and Ranging

RPA - Remotely Piloted Aircraft

SLAM - Simultaneous Localization and Mapping

T/ha - Tonnes per Hectare

TLS - Terrestrial LiDAR Scanner

UAV - Unmanned Aerial Vehicle

UV – Ultra Violet

Positionality Statement

I held a MITACs internship opportunity with Korotu Technology from May 2022 to October 2023. During this period, I engaged in in-situ data collection as part of my work for Korotu's CarbonWatch module. This internship allowed me to gain hands-on experience and a deeper understanding of Korotu's technologies and objectives. I contributed to the development and testing of DroneWatch, an application that supports forest monitoring efforts. My involvement in this project provided insights into how the software functions and its integration with other tools.

The research I conducted during my time at Korotu was mutually beneficial, providing both Korotu and my academic work with valuable outcomes. For Korotu, the field data collection and the development of biomass and carbon monitoring software enhanced the accuracy and applicability of their products, improving their ability to deliver precise forest biomass estimates and carbon metrics. Simultaneously, the insights and data gathered directly supported my thesis, which focuses on quantifying the distribution of above-ground biomass estimates in forested areas across LiDAR applications and multiple scales. During my experience at Korotu, examining the practical applications of in-situ data sampling alongside LiDAR-based methodologies motivated me to explore how accuracy and reliability can vary according to specific project requirements.

This collaboration not only contributed to the advancement of my own research but also added to the broader scientific understanding of LiDAR technologies in forest biomass quantification. By integrating in-situ data collection with innovative software development, the work supported efforts to enhance the accuracy of carbon monitoring systems and forest management practices. This synergy underscores the importance of industry-academic partnerships in advancing technology and scientific research.

While my work with Korotu has shaped my expertise in remote sensing and spatial data analysis, I remain committed to maintaining objectivity and providing unbiased analysis throughout my research endeavors. This partnership has provided me with unique insights into technological advancements in forest monitoring, contributing both to my academic growth and to the ongoing development of cutting-edge tools in the field of environmental science.

First Chapter – A Primer on LiDAR

1.1 LiDAR Background

LIDAR (Light Detection and Ranging) is a remote sensing technology capable of determining the distance travelled between an object and the sensor by utilizing Light Amplification by Stimulated Emission of Radiation (LASER) pulses, which are pulses of narrowed beams of light to calculate the approximate duration it takes photons to travel to an object and return to the sensor (Xiaoye Liu, 2008). LiDAR systems consist of 3 main components, the laser scanner system that actively sends out pulses of light typically ranging from the ultraviolet (UV) through the visible spectrum and extending into the near-infrared (NIR) region, approximately 0.2 μm to 1.6 μm. This extensive wavelength range allows LiDAR systems to be customized for various applications, including topographic mapping, vegetation analysis, and biomass estimation (Carson et al, 2004), with commonly employed laser systems including Nd:YAN lasers, diode lasers, fiber lasers, semiconductor lasers and CO_2 lasers that vary in cost, accuracy, range and mobility; a Global Navigation Satellite System (GNSS) receiver to record relative position in space; and an Inertial Measurement Unit (IMU) to measure the motion and attitude of the sensor (Xiaoye Liu, 2008; Sharma et al, 2010).

The benefits of LiDAR applications over traditional surveying methods can be distilled into one key factor: speed. LiDAR can collect between 10,000 – 2,000,000+ points per second, a rate of which would take traditional surveying years to record at the same level of detail. A ground-based LiDAR system, fixed in position, is able to shoot photons that travel at the speed of light (c, approximately 3x10^8 m/s in a vacuum) and the time until the photon's return is used to calculate the distance between the sensor and the feature of interest (e.g., Distance = flight time * c/2). A different approach can also be used to calculate the distance between the sensor and a feature utilizing an amplitude modulated continuous waveform laser (AMCW), where the light intensity is adjusted but the frequency of the laser is constant (Torun et al, 2019). In the AMCW process, when the beam hits an object, the phase is reset, and the return signal is processed alongside the flight duration to calculate the distance at a much greater accuracy than its time of flight only counterpart albeit at much lower range (Torun et al, 2019). The calculations are straightforward due to the originating photons placed at a known and fixed position, but when LiDAR systems are placed on mobile platforms such as backpack-based LiDAR Simultaneous Localization and Mapping (SLAM) systems, remotely piloted aircraft (RPA)/aerial LiDAR systems, and even Satellite based LiDAR systems, the accuracy and determination of distance is substantially more complicated (Fowler et al, 2000).

Mobile LiDAR systems can cover large swaths of land with great detail compared to older mobile surveying methods such as RADAR (Radio Detection and Ranging) (Bauwens et al., 2016). For example, in the case of a LiDAR sensor affixed to a plane, the IMU can determine the azimuth angle (horizontal) and elevation angle (vertical) to get a three-dimensional view (Peinecke et al., 2008), whereas RADAR would only provide a 2D representation (de Badereau et al., 2003). LiDAR Systems on mobile platforms (i.e., those without a fixed position) require accurate determination of their position in space when photons from the lasers are emitted and returned to calculate the approximate time and distance travelled. Attributes such as relative position, acceleration, angular velocity, tilt, and beam strength play a large role in determining the accuracy of measurements and as such need to be considered and can be measured using a GNSS receiver and IMU on the LiDAR System (Fowler et al, 2000; Woods & Christian, 2016; Xiaoye Liu, 2008). These attributes can be simplified into three main components: 1) Inertial Translation state, provided by a GNSS, gives the position and velocity of the device holding the sensor; 2) Inertial Attitude, the orientation or angular position of an object in space is retrieved using a star tracker; and 3) Relative Pose, is the spatial relationship between two objects (the sensor and a known object/reference) and it is typically mathematically derived using models to match the LiDAR sensed images to references and/or objects allowing for transformations to be made to match the reference (Fowler et al, 2000; Woods & Christian, 2016). The speed, spatial range and accuracy of LiDAR systems can be used to provide valuable insights for forestry applications (Coops et al., 2021).

1.2 The Role of LiDAR in Forest Management

Understanding and quantification of forest metrics is vital to making informed decisions on the management, procurement, and securement of forested areas (Falkowski et al., 2009). The assessment of forest metrics (e.g., biomass) needs to be measured at a level of accuracy to best match the fidelity required for a project (e.g., land securement, year over year biomass change analysis). Biomass is the total mass of an organism and in the context of vegetation can be a significant indicator of change of forest growth and carbon storage potential over time (e.g., forest development after disturbance events) (Brown et al, 1997; Dube et al, 2018). By evaluating the change in biomass and storage potential over time, it is possible to better understand how forests development may have been in the past, present, and future. Biomass and carbon have a direct relationship where 1 unit of biomass equates to 0.45 - 0.53 units of carbon (e.g., Negi et al, 2003; Petersson et al., 2012; Pradeep et al, 2024), for the purpose of this research a biomass to carbon conversion factor of 0.5 will be utilized following IPCC (Intergovernmental Panel on Climate Change) recommendations (IPCC, 2003, Chapter 3.25; Petersson et al., 2012). The amount of carbon may be transformed into a Carbon dioxide equivalent value, a common unit value by using a

conversion factor of 3.67 (US EPA, 2015). Biomass and carbon values can be represented as various pools within a forest ecosystem including soil carbon, below ground biomass (BGB) which includes root systems, dead plant material such as the non-living components of fallen over trees, and AGB that includes the amount of live or dead matter in woody vegetation, mostly in the trunks, stems, and foliage of trees. In-situ assessment of AGB can be calculated destructively using the dry weight of trees/shrubs after cutting trees down or non-destructively by applying allometric equations by getting relationships between different tree parameters (Kumar & Mutanga, 2017), although allometric equations are originally derived from destructively sampled trees through oven-drying, the relationships identified from the measured biomass components allow for the estimation of AGB without further harm to forest life.

The change in biomass can be a significant indicator of overall forest productivity and fluctuations in carbon storage potential (Brown et al, 1997; Dube et al, 2018; Wang et al, 2010). Biomass increases may occur due to favorable climate and soil conditions, while decreases often signal disturbance events (e.g., logging, invasive species, forest fires) or intensified competition, but highly accurate estimations of AGB through current industry standards (e.g., in-situ measurements) can be costly and/or tedious to measure as it requires large amounts of resources as a function of the spatial coverage required for the project in question. Traditionally, data collection on above ground biomass is conducted in-situ with foresters going out into the field and conducting tree inventories using fixed radius (e.g., Vegetation Sampling Protocol; (Vegetation Sampling Protocol (VSP), n.d.) or variable plots using a wedge prism or angle gauge (Stuart, 1984). In-situ data collection is incredibly time consuming, resource intensive, and costly while lacking the facility for continuous monitoring (e.g., personal experience, it took four full workdays [8 hours per day] to assess 22 8m-radius plots across three sites with a team of five).

While in-situ measurements are invaluable for forest assessment and management, it's important to recognize and mitigate sources of error. Height measurements using clinometers are both tedious and susceptible to human error often showing underestimation of absolute tree heights (Martin, 2022) on account of incorrect angle readings, sloped terrain, baseline measurement errors, or inaccuracies in identifying treetops. This inaccuracy in height measurements by clinometers can further propagate and impact the accuracy of allometric equations developed to use both diameter at breast height (DBH) and tree canopy height. When considering the practicality of measurements, DBH alone is a reliable predictor of biomass (Xiang et al., 2016). However, measurements in DBH can also introduce errors on account of measuring on sloped terrain, differing height levels, and general user error. Still, determining DBH typically requires less specialized knowledge than more complex metrics, such as assessing tree health or identifying species, which demand a deeper understanding of forest systems. While measuring tree height in situ can involve significant potential for error—averaging an underestimation of 20% (Larjavaara & Muller-Landau, 2013)—the error rates for DBH measurements are considerably lower. Specifically, DBH

measurements exhibit only about a 1.5% deviation when comparing various measurements of the same tree with only 5% of cases with greater than 5% of DBH difference (Luoma et al., 2017). By adopting DBH-only or DBH-canopy width-based allometric equations, the reliability of biomass estimations can be enhanced particularly when height measurements are unreliable, ensuring more accurate assessments of tree biomass and other ecological parameters across in-situ and LiDAR-based measurements.

LiDAR technology offers an alternative method to traditional in-situ data collection that can be applied across large spatial extents, but can also be costly (Wulder et al, 2008). LiDAR data can be collected at multiple scales/platforms (distance above ground level [AGL]): terrestrial LiDAR [0-2m AGL], RPA LiDAR [~60m AGL], aerial LiDAR [~2000m AGL], and satellite-based LiDAR such as the Global Ecosystems Dynamic Investigation (GEDI) module aboard the International Space Station. These various scales produce different levels of data accuracy and cost that can meet specific project requirements without creating data redundancy. By assessing the 3D vertical structure of forest landscapes, collected by the LiDAR sensors, it is possible to extract forest metrics such as DBH, tree height, and canopy width to quantify the amount of biomass and carbon stock in forested areas. Improvements in LiDAR technology will continue to propel the efficiency and accuracy of LiDAR-based forest biomass assessments.

Early LIDAR systems had limited pulse rates and point densities, resulting in sparse measurements. Modern sensors, however, operate at much higher pulse rates, generating dense point clouds that capture fine details of forest structure, and will continue to improve with time. Additionally, the miniaturization of sensors now allows integration with UAVs, providing high-resolution data at lower costs (Hu et al., 2021). As technology advances, LiDAR's role in forest management and conservation efforts will become more indispensable (Beland et al., 2019).

In this study, we utilized the Riegl miniVux1 LiDAR system, which operates within a more specific wavelength range of 0.8 μm to 1.6 μm. This narrower band was deliberately chosen for biomass assessment for several key reasons. The 0.8 μm to 1.6 μm wavelengths enhance vegetation penetration, as it is more conducive to reflectance from vegetation, enabling more accurate measurements of both canopy structure and underlying vegetation layers, which is essential for precise biomass estimation. This specific wavelength also coincides with established vegetation indices like the Normalized Difference Vegetation Index (NDVI), that rely on red and NIR bands, allowing compatibility between LiDAR and other remote sensing databases.

Forest metrics such as biomass can also be calculated using other remotely sensed products such as NDVI which reflects vegetation vigor and density. By applying field measurements of biomass to NDVI values, it becomes possible to fit linear regression models to estimate biomass (Cabrera-Bosquet et

al., 2011). However, approaches using vegetation indices are challenged by complex stand structures and environmental conditions that limit the accuracy of estimations (e.g., closed canopies or dominant trees towering over the study area limits the amount of information present for understory vegetation). Conversely, use of high point density LiDAR can facilitate a more accurate reconstruction of the 3D vertical structure of trees to better understand these complex structures (Wang et al, 2010) where NDVI may be lacking. LiDAR also holds an advantage over photogrammetry when assessing areas with closed forest canopies in which LiDAR can more accurately assess ground values (Almeida et al, 2019). By harnessing the power of LiDAR systems, automatic forest inventories can be conducted, and forests can be more efficiently monitored (Almeida et al, 2019; Chen & Zhu, 2013). Each LiDAR platform can collect varying amounts of data in terms of point density (the number of points the LiDAR unit sends out per unit area, typically in square meters), costs and overall accuracy as a result of the sensor and height of data acquisition. For example, the level of vertical and horizontal accuracy can vary between satellite-based LiDAR and aerial LiDAR due to technical limitations such as beam strength and signal loss (Marian et al, 2016). Ultimately, the usage of LiDAR allows the processing of its raw data to constitute various depictions of biomass estimation accuracy depending on the scale, point density, and elevation (AGL) that is employed. While LiDAR can be used to estimate AGB, it cannot directly estimate soil and litter biomass pools, leaving some components of forest ecosystems unrepresented. Understanding the error rates and accuracies between various LiDAR height strata's (e.g., terrestrial, RPA, aerial, and satellite-based LiDAR) allow for more informed decision making on small and large spatial scales, and the appropriate platform to utilize for specified project requirements.

Chapter 2, aligned with the overarching goal of this thesis, aims to quantify the variation in forest biomass estimation from multiple remote sensing approaches and compare their accuracy relative to in-situ measurements. Understanding the error associated with different remote sensing approaches can improve our understanding of carbon estimates, better harmonize results from different approaches for comparative analyses, and ideally, aid the securement, monitoring, and protection of forested areas in Canada to protect biodiversity, cost effectively and accurately. To achieve this goal, I seek to answer the question: to what degree are remotely sensed data estimates of biomass consistent with coincident (i.e., spatial and temporal) in-situ assessments. In turn, I seek to answer how can LiDAR-based estimates of aboveground biomass be used to monitor the success of nature-based solutions for mitigating and adapting to climate change and if GEDI is accurate enough to make carbon assessments? This will be done by assessing the accuracy of RPA LiDAR, aerial LiDAR, and Satellite LiDAR assessments against in-situ forest metrics (i.e., biomass) across ten 8m radius plots spread across 2 properties within the Kawartha Region of Ontario, Canada.

In Chapter 3, potential future directions for the integration of LiDAR technology in forestry is discussed, which involves additional types of data that can enhance the research in Chapter 2, such as stem count and species identification. Chapter 2 does not cover the use of terrestrial LiDAR or satellite-based systems like ICESat-2, both of which could offer important insights and significantly broaden the spatial coverage of LiDAR-based measurements. For instance, ICESat-2 could help in estimating biomass in regions beyond GEDI's operational latitude range of 51.6 degrees north and south. The inclusion of such technologies and additional data layers may provide a more comprehensive understanding of forest ecosystems.

Despite growing awareness of the benefits of Nature-based Solutions (NbS) in mitigating and adapting to climate change, their uptake has been slow due to a lack of funding. This stems from a lack of confidence due to literature gaps on the long-term practicality of NbS, due to the concern of requiring continuous monitoring to ascertain benefits and co-benefits (Chausson et al., 2020). This continuous monitoring is resource intensive and costly, especially on projects of large magnitudes and spatial scales. By utilising remote sensing to calculate biomass and carbon stores, it is possible to conduct monitoring of areas at both a cost-effective rate and at a much higher temporal resolution. However, to accurately interpret the results, it is crucial to understand the error rates of different LiDAR apparatus and point density scales. By improving confidence in the effectiveness of NbS projects through accurate and cost-effective monitoring, funding for these initiatives can be increased, ultimately helping to mitigate and adapt to climate change more effectively.

Chapter 2

1 Introduction

Over the past few decades, the rapid growth of remote sensing technologies has transformed how we capture and analyze environmental data at large spatial scales. Among these methods, LiDAR (Light Detection and Ranging) stands out for its remarkable precision and versatility (Weng, 2011). LiDAR is a remote sensing technology that harnesses the power of a laser (Light amplification by the stimulated emission of radiation) as a measurement tool with high precision (Weng, 2011). LiDAR has been utilized across a spectrum of applications from measuring topography (e.g., Mallet & Bretar, 2009), quantifying erosion (e.g., Meinen and Robinson, 2021), recording building facades (e.g., Haghighatgou et al., 2022; Peethambaran & Wang, 2017; Truong-Hong & Laefer, 2014), measuring object heights and volumes (e.g., Nilsson, 1996), and measuring forest characteristics and biomass (e.g., Coops et al., 2021; Popescu et al., 2003). LiDAR involves leveraging laser properties, including but not confined to wavelength, beam strength, and duration (Weng, 2011) to calculate metrics such as the distance travelled from the emitting laser/sensor which can then be further processed to derive three-dimensional (3D) models (e.g., topography, Xiaoye Liu, 2008; buildings, Peethambaran & Wang, 2017). LiDAR has revolutionized geographic data collection that exceeds previous measurements methods such as surveys and photogrammetry who hold high precision but tend to be both time consuming and labour intensive (Xiaoye Liu, 2008). With LiDAR, data can be collected from large swaths of land while reducing the cost and labour required relative to more traditional methods such as in-situ data collection, allowing for better repeatability of measurements. The need for collecting data across large areas with greater repeatability for accurate assessment of change over time is prevalent in biomass estimation of forested areas, where LiDAR data is capable of being processed to create 3D vertical structures of forest environments allowing for the calculation of tree metrics at an unprecedented speed compared to traditional methods (e.g., dry-weight sampling, Brandeis et al., 2006; forest inventories, Chave et al., 2019).

Traditionally, biomass estimation of forested environments is done in-situ with foresters measuring tree characteristics (e.g., DBH, species, height, geolocation, dominance, canopy size, health status) using fixed-area or variable plots (plots with no specific area measuring only trees that are counted as ‘in’ using an angle gauge or wedge prism). These measurements are then used to calculate biomass and carbon (C) stock using allometric equations. Allometric equations represent a statistical relationship between the growth of an object (in this case a tree) and a measurable characteristic (in this case the trees diameter at breast height). The specificity of allometric equations can be high such that they are species-specific (e.g., red maple, Lambert et al., 2005), moderate such that the equations are applied at the level of

genus (e.g. maple, Flade et al., 2020), generalized for application at the forest stand level (e.g., broadleaf, coniferous, or mixed wood), and even broad for applications to larger areas with more ambiguity (e.g., plant function types (PFTs) covering continents used by GEDI) (Duncanson et al., 2022). The benefit of the generalization of allometric equations is that it allows for the estimation of biomass where tree species identification information is not available (Paul et al., 2013).

Although, traditional biomass estimation methods (e.g., in-situ forest inventories using species specific regional allometric equations) provide biomass estimates with less than 11% error when applying regional species level allometric equations based on southern and eastern Australia (Paul et al., 2013) compared to oven dried biomass estimates in a laboratory setting, they are time consuming, labour intensive and costly. For example, in-situ measurements for 10 easily accessible 400m^2 plots was quoted at $6200 CDN in southern Ontario. The main costs included $4,375 for field work (DBH, species, status, and height measurement), $350 for background review (e.g., identifying plot locations), $131.25 for administration, $437.50 for data consolidation, and $175 for final coordination—all subject to HST and disbursements. Any additional services, such as extra field studies or wildlife assessments were not included and would be billed separately at hourly rates. As a result, due to logistical and practical constraints, comprehensive in-situ surveys of larger forests spanning 100s of hectares becomes challenging. In lieu of assessing the entire forest area, forest inventories are conducted using representative plots which are then interpolated to estimate biomass values across the entire forest landscape (e.g., Fleming et al. 2015). A low number of representative plots can introduce bias to estimates calculated for larger areas as they cannot fully account for environmental heterogeneity, this issue is exasperated when remeasurements with sufficient temporal resolutions are required (Liang et al., 2018), LiDAR alleviates much of these concerns as it can reduce the cost, time and labour required significantly while allowing repeatability for AGB estimates but lacks the ability to assess other carbon pools within soil and litter. Depending on the scale of the LiDAR measurement (e.g., Terrestrial, RPA, Aerial, Satellite), the technology enables scanning of large swaths of forests eliminating or reducing the need for interpolation, a method typically employed to estimate values of unmeasured areas between known points of value.

LiDAR systems come in two main types: flash-based and non-flash-based. Flash-Based LiDAR quickly covers an area by emitting a wide, simultaneous burst of light, similar to a camera flash. This method generally captures extensive data with minimal gaps, often eliminating the need for data interpolation. Interpolation is a process used to estimate missing data within a survey area.

Non-Flash-Based LiDAR sends out laser beams in narrow, fixed-radius "shots" that target specific points on the ground. Shot radiuses define the spread of a single photon or beam when it hits the ground and can vary depending on the LiDAR sensor and height of the measurement above ground level

(AGL). This focused approach can leave gaps in data coverage, especially in uneven terrains or dense vegetation, necessitating the use of interpolation to fill in these gaps and provide a complete analysis of the area

Interpolation is often necessary in traditional forest inventories and Non-Flash-Based LiDAR where data points are sparse, but the comprehensive coverage by Flash-Based LiDAR helps to ensure that more of the forest is directly measured.

Despite its advantages, the accuracy of LiDAR based biomass estimations call for concern. LiDAR data collection is the first step in assessing forest biomass. However, collected data need to have outliers (noise) removed and georeferenced and processed to generate a canopy height model. The tree heights can then be used to estimate DBH (e.g., Buba, 2013; Özçelik et al., 2018), a required input of the aforementioned allometric equations. The granularity (i.e., pts / m^2) of LiDAR data can vary by acquisition sensor and flight parameters, which along with different data processing workflows can yield different biomass estimates. Therefore, LiDAR estimates require in-situ ground truth measurements to calibrate and validate remote-sensing-based estimates (Vaglio Laurin et al., 2014). In-situ estimates are still considered the most accurate non-destructive measurement methodology (Liang et al., 2018; Paul et al., 2013) and statistical approaches (regression, Li et al., 2008) and machine learning models (random forests, Li et al., 2019) are often used to establish numerical relationships between in-situ measurements and remotely sensed LiDAR based forest metrics.

In forest applications, LiDAR provides high density data that, once processed, can provide geolocated treetops, tree count, tree height, and canopy diameter data. These data can be further processed to estimate tree DBH, biomass, and basal area. LiDAR data collection of forests can be conducted on multiple scales (distance above ground level [AGL]): from Terrestrial LiDAR Scanning (TLS) [0-2m AGL], utilizing simple mobile devices to more sophisticated on the ground sensors (e.g., Leica Multistation, Meinen and Robinson 2020), RPA LiDAR [~50-120m AGL] utilizing drones (e.g., Novo-Fernández et al., 2019), aerial LiDAR [~2000m AGL] utilizing planes or helicopters (e.g., Li et al., 2024), and satellite-based LiDAR such as the Global Ecosystems Dynamic Investigation (GEDI, Dubayah et al., 2020) module aboard the International Space Station (ISS). All scales of LiDAR offer similar forest measurement outputs, but to date, there is no literature offering a comparison across these scales to understand how these platforms affect estimates of AGB biomass in forest.

Comparing forest measurements from LiDAR data across multiple scales of acquisition can improve our ability to quantify accuracy and its variation relative to the cost, time, and repeatability of data acquisition. The outcome of comparative studies not only increase the decision-making capacity of stakeholders considering similar applications, but they can also identify challenges or gaps that require invention or innovation to achieve specific scientific or societal needs that have not been met. In the case

of analyzing an individual plot at an easily accessible location, a terrestrial LiDAR scan may prove to be the best solution by combining providing high density point clouds with a relatively low cost, but such an approach is infeasible for a comprehensive forest inventory across a large spatial extent. A property manager with multiple smaller forested areas (e.g., plantations) may benefit from utilizing RPA based data collection to keep track of biomass change over time while national assessments of forests would benefit from satellite-based approaches to cover the magnitude required. However, the degree to which these different approaches to biomass and carbon estimation vary or compare to in-situ based measurements remains unknown.

The presented research contributes to closing the gap in multi-scale comparison of forest biomass estimation by comparing in-situ to RPA, aerial, and satellite-based measurements. The multi-scale comparison is applied across two southern Ontario forests located in the Kawartha region in which biomass was assessed using in-situ (fixed plot), RPA-based LiDAR, Aerial LiDAR, and GEDI. Comparing forest measurements from LiDAR data across multiple scales can improve our understanding of accuracy, costs, and the feasibility of frequent data collection. However, to what extent do biomass estimates derived from different LiDAR platforms, spanning RPA, aerial, and satellite, align with or deviate from conventional in-situ measurements? This core question guides the present research, which aims to evaluate the accuracy of multi-scale LiDAR-based biomass estimates relative to in-situ methods and assess the associated cost–benefit trade-offs.

2 Methods

2.1 Study Area

The study comprises two sites located within Great Lakes-St. Lawrence Forest ecoregion of southern Ontario, characterized by its diverse temperate forests and wetland ecosystems. The selected sites are Ballyduff Trails (105.8 ha, 44.1436°N, 78.6215°W, Figure 2.1) and Christie Bentham Wetland Trails (55.4 ha, 44.5470°N, 78.1957°W, Figure 2.2). Ballyduff trails is an area that borders Fleetwood Creek Natural Area and contains a mixture of softwood, hardwood, and mixed-wood forests as well as some area in wetlands. As part of the glacially formed Oak Ridges Moraine (*Ballyduff Trails (McKim-Garsonnin) - Kawartha Land Trust*, 2023), the topography varies between 264 and 353 m above sea level and consists of rolling hills, sand deposits and a wetland. The area within which Ballyduff resides is primarily agriculture with a low population density. Ballyduff Trails was originally used for sustenance farming in the mid-19th century by European farmers but was put into residential land use by a single owner in 1986. This owner has been trying to restore the ecological integrity of the property, meaning the condition in which the ecosystem's composition, structure, and process remain functioning and resilient

through measures such as annual tree planting, establishing a native prairie, while simultaneously opening the property for recreational use (e.g., nature walks, cross-country skiing, snow shoeing). The property has taken several initiatives to restore ecological integrity including the planting of white pine and red oak annually, establishing a native prairie, creating wildlife habitats, controlling invasive species, and protecting the existing wetland. In 2011, Ballyduff Trails became protected under a conservation agreement with Kawartha Land Trust (KLT).

In the surveyed area of 0.14 hectares done in-situ in Ballyduff, 117 trees were identified across ten species. scott pine (*Pinus sylvestris*) was the most prevalent, accounting for 24% of the trees with 28 individuals. Eastern white cedar (*Thuja occidentalis*) was the second most common, comprising 22% with 26 individuals. Trembling aspen (*Populus tremuloides*) made up 15% of the sample with 18 trees, followed by sugar maple (*Acer saccharum*) at 13% with 15 individuals. American hophornbeam (*Carpinus caroliniana*) accounted for 8% with 9 individuals, and ironwood (Ostrya virginiana) represented 7% with 8 trees. Other species present in smaller quantities include paper birch (*Betula papyrifera*), red oak (*Quercus rubra*), eastern white pine (*Pinus strobus*), and big tooth aspen (*Populus grandidentata*).

The second study area, Christie Bentham Wetland Trails (previously known as Clear Lake North Wetland), is located in Selwyn, Ontario, and is managed by the Kawartha Land Trust. Despite the name of this property, the portion residing in wetland (found solely in the southeast) is minor relative to a diverse set of forest stands in its upland area that includes mixed wood, broadleaf, coniferous and shrublands. The topography varies from 199 m to 254 m above sea level. Christie Bentham Wetland Trails sits on a bedrock of limestone throughout the property showcasing the history of the residing glaciers via plentiful fossils and erosion channels within the limestone. The forest environment is dominated by Juniper meadows and Hemlock forests.

In the surveyed area of 0.06 hectares, 63 trees were identified across five species. Ironwood (*Ostrya virginiana*) was the most prevalent, accounting for 46% of the trees with 29 individuals. Sugar maple (*Acer saccharum*) was the second most common, comprising 38% with 24 individuals. Eastern white cedar (*Thuja occidentalis*) made up 10% of the sample with 6 trees, while both eastern white pine (*Pinus strobus*) and white oak (*Quercus alba*) each represented about 3% with 2 trees each.

Although this survey covers only 0.11% of the total 55.5-hectare property, it provides initial insights into the forest composition. The dominance of Ironwood and Sugar Maple suggests that the environmental conditions in the sampled area favor these species. However, harvesting or historical management practices might also have selectively reduced other tree species, inadvertently reinforcing ironwood and sugar maple dominance in the plots surveyed. Because of this limited scope and the

possibility of varied land-use history across the property, these findings may not fully represent the overall species distribution.

(a)

(b)

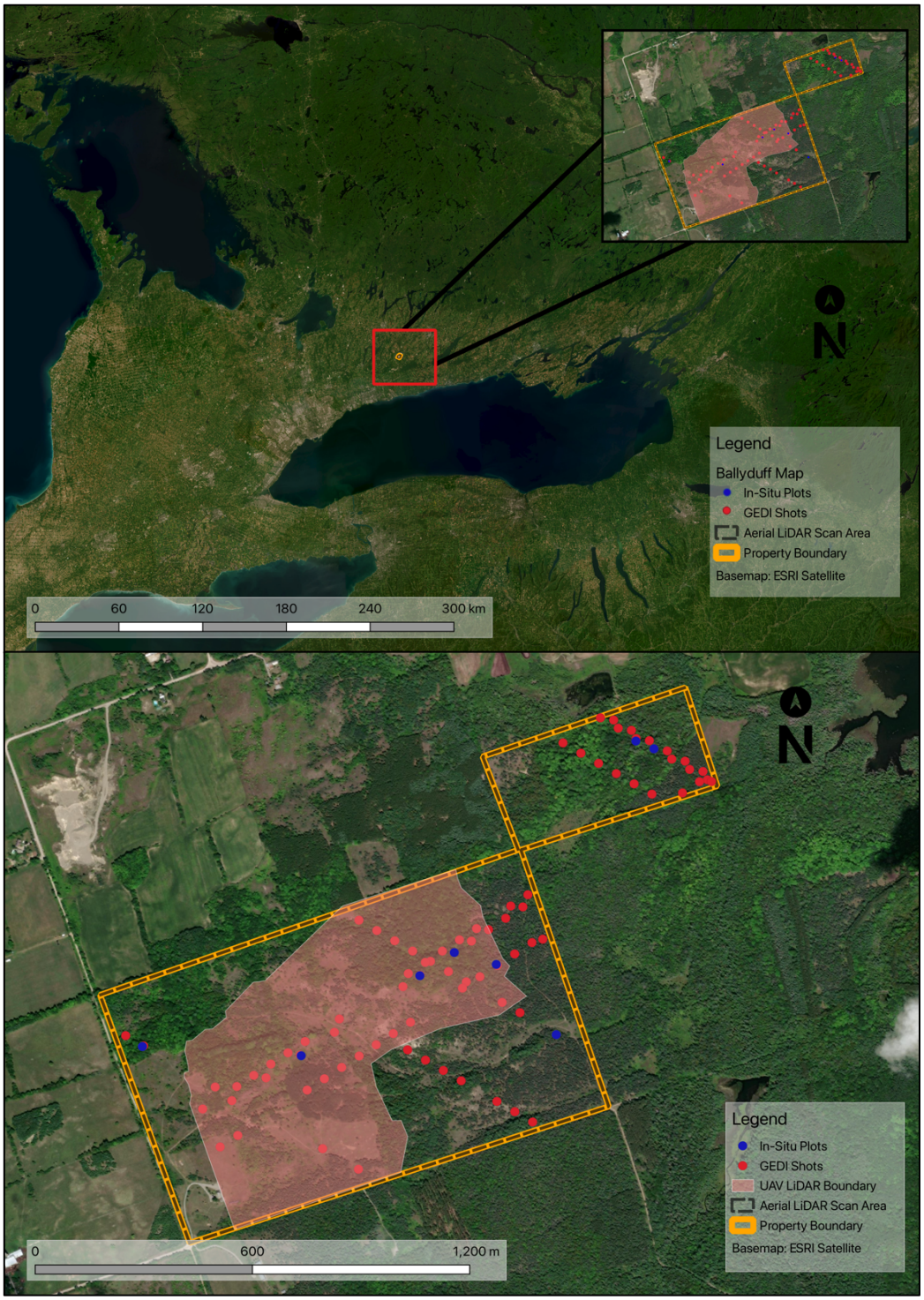


Figure 2.1 (a) An inset map showing the location of the Ballyduff Trails study area within Ontario, offering a regional context for the research site (b) A detailed view of the Ballyduff Trails study area, highlighting the in-situ plots, GEDI shots, UAV LiDAR scan area, and Aerial LiDAR scan area. The outlined property boundary is also visible within the broader forest landscape.

(a)

(b)

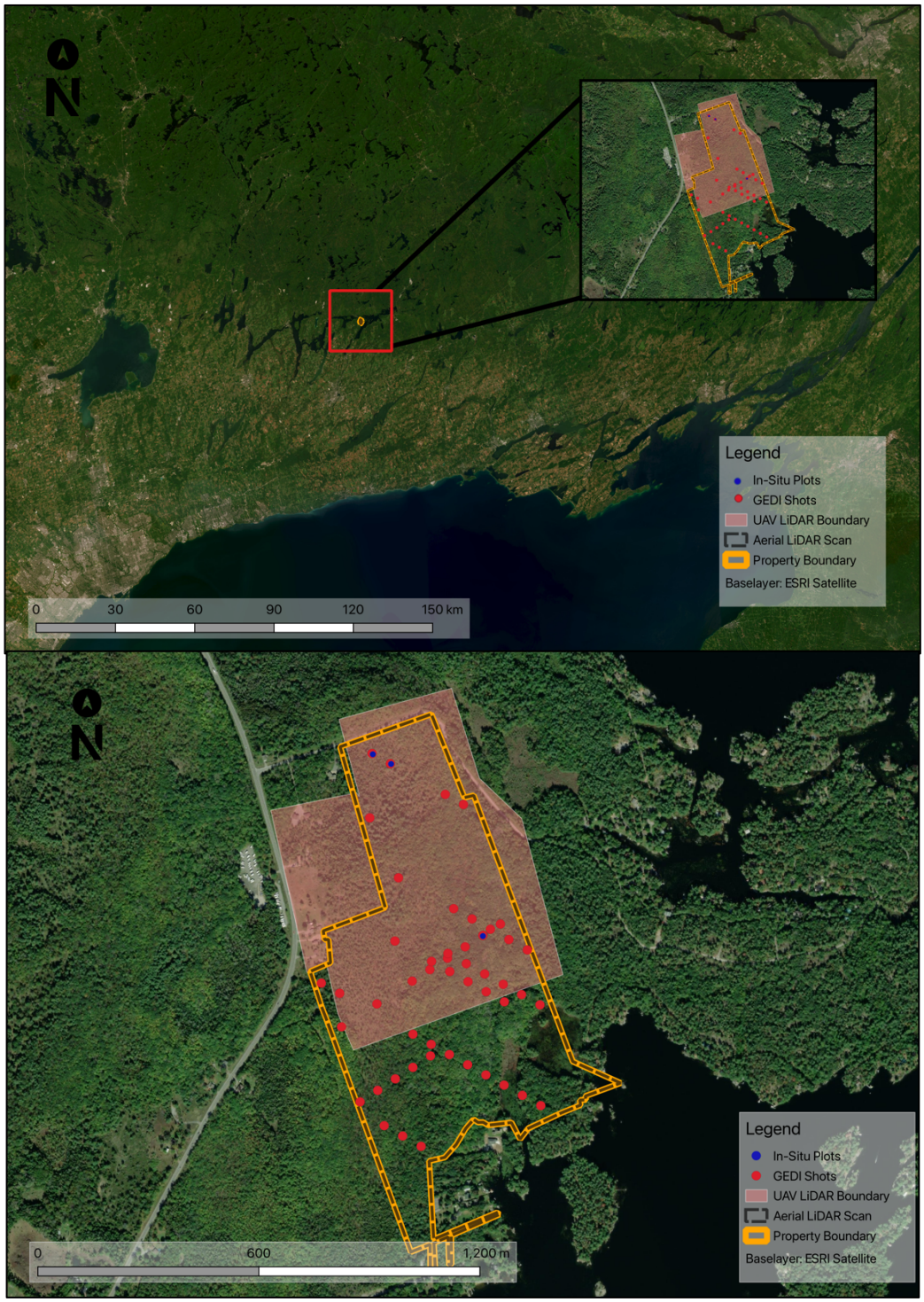


Figure 2.2 (a) An inset map showing the location of the Christie Bentham Wetlands study area within Ontario, offering a regional context for the research site (b) A detailed view of the Christie Bentham Wetlands study area, highlighting the in-situ plots, GEDI shots, UAV LiDAR scan area, and Aerial LiDAR scan area. The outlined property boundary is also visible within the broader forest landscape.

2.2 Data

2.2.1 Data Processing

Tree metrics and biomass estimates were made at two spatial scales (in-situ site level and the larger study site level) using in-situ, RPA, aerial, and satellite (i.e., GEDI) LiDAR data. Given the range of spatial resolutions and areal coverage of the data acquired from the different sensors, several methods were used to harmonize their data for comparative purposes. Since biomass estimations from in-situ plots and GEDI footprints only cover a small area (201 m^2 and 491m^2, respectively) and are sparse in coverage, interpolation was used, at 1-hectare increments, to derive and estimate biomass for the entire property parcel. Two interpolation methods were used: inverse distance weighted (IDW) interpolation and tree-stand-based averages, where the average of forest stands with observational data were applied to similar forest stands lacking observations. Tree stands are groups of trees that carry similar characteristics, and their definition may be as coarse as deciduous or coniferous (Spinelli et al., 2016) or incorporate more specificity by using characteristics such as age, species type, and composition (spread/density, e.g., Spinelli et al., 2016).

For clarity in this research, the term "biomass" refers exclusively to AGB in forested areas, measured from standing trees with a DBH of at least 6 cm and a minimum height of 2 m. Other biomass and carbon pools, such as soil and litter, are not considered in this assessment.

Metrics such as basal area and tree height were calculated using basic geometric principles. Basal area, which represents the cross-sectional area of a tree trunk at breast height, was calculated by applying the formula for the area of a circle using DBH:

$$BA = \pi \left(\frac{DBH}{2}\right)^2 \tag{2.3}$$

Equation 2.3 Formula for basal area (BA), where DBH is the diameter at breast height

Meanwhile, tree height was estimated through simple trigonometry, measuring the horizontal distance from the observer to the tree and the angle to the top of the tree, while also accounting for any elevation difference between the observer and the base of the trunk. Biomass estimates were calculated using DBH based allometric equations mainly from Chojnacky, Heath & Jenkins (2014). Where these equations were not applicable, alternative localized or generalized models were utilized, integrating both height and DBH measurements when necessary. Allometric equations that also incorporated tree height were tested, but given similar results and fewer species-specific equations, we opted for equations that only required DBH. For individual tree species that could not be identified, Canada wide generalized, as well as forest stand (hardwood, softwood, mixed wood) generalized (where forest stand information is

available) allometric equations from Lambert et al. (2005) were utilized. In-situ field data collected in smaller 8m radius plots were scaled up to one-hectare representations to match LiDAR based biomass estimations represented as 1-hectare grids (e.g., GEDI).

This study employs a comprehensive data collection strategy spanning several years and multiple locations. From 2016 to 2023, various methodologies were implemented, including Aerial LiDAR surveys, GEDI data acquisition, in-situ measurements, and RPA LiDAR deployments. Figure 2.4 provides an overview of the timeline, illustrating the sequence and overlap of these data collection activities essential for the thorough analysis of the Ballyduff Trails and Christie Bentham Wetland Trails ecosystems.

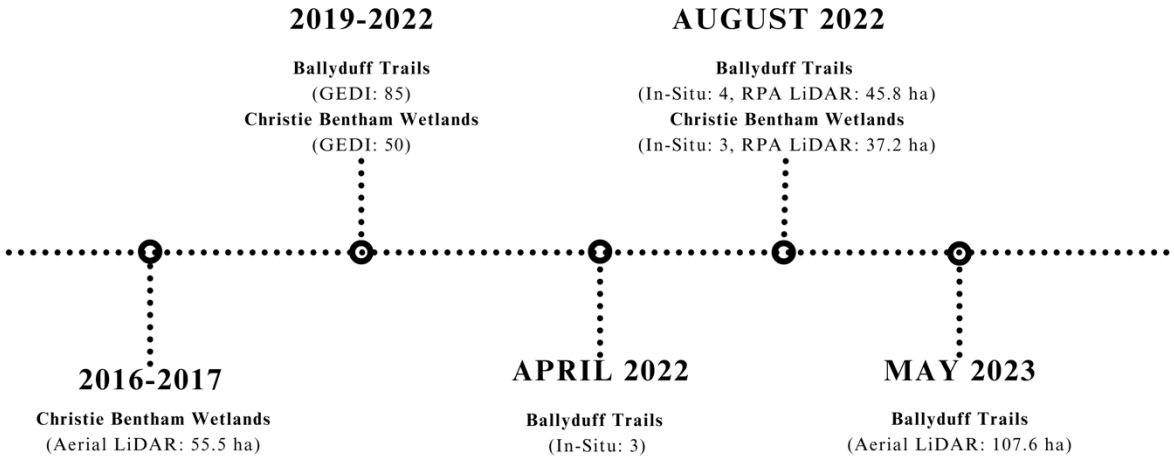


Figure 2.4. Timeline illustrating the collection of remote sensing and in-situ data at the Ballyduff Trails and Christie Bentham Wetland Trails study sites. Aerial LiDAR was first acquired at Christie Bentham Wetland Trails in 2016–2017, followed by GEDI data acquisition at both sites from 2019–2022. In April 2022, 3 in-situ measurements were collected at Ballyduff Trails, and in August 2022, both in-situ measurements (Ballyduff Trails: 4, Christie Bentham Wetland Trails: 3) and RPA LiDAR were collected at the two sites. Most recently, Aerial LiDAR surveys were conducted at Ballyduff Trails in May 2023.

2.2.2 In-situ Data Collection

In-situ data were collected using 8m radius fixed plots with all standing trees with a DBH of 6 cm or more and a minimum height of 2m within the radius contributing to the total aboveground biomass within the plot (Figure 2.5). Plot centers were chosen to reside within interior forest situated 50 m from forest edges to reduce edge effects while encompassing diverse forest types. These locations were pinpointed by the field crew within the forest by triangulating with multiple mobile GPS devices with a horizontal accuracy of 5-10 m (Technologies, 2020). The following measurements were collected: tree species, DBH at a height of 1.3m from the base of the trunk, distance of the tree from the plot center, tree

dominance (e.g., understory, co-dominant or dominant), site conditions (e.g., rocky terrain, south facing slope), and distance/angle to dominant trees from the plot center.

A total of 7 plots (0.14 ha total area) were assessed in Ballyduff in 2022 spread across two missions (3 conducted on April 30th and 4 conducted on August 12th). These 7 plots included: 3 coniferous, 3 deciduous and 1 mixed-wood forest stand. Conversely, 3 plots (0.06 ha total area) were evaluated in Christie Bentham on August 11th of 2022, with 2 mixed-wood and 1 deciduous forest stand.

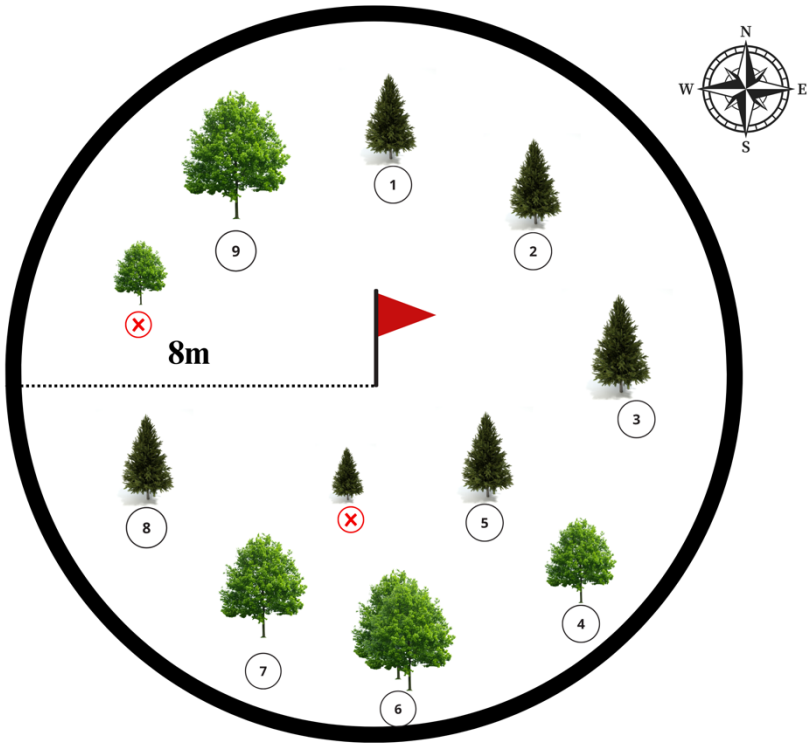


Figure 2.5. Schematic of in-situ data collection. First, each pre-determined plot center is geolocated with a mobile GPS device. An 8 m radius from the center defines the circular plot boundary. True north (0°) is established, and all trees ≥6 cm DBH and ≥2 m in height are measured by moving clockwise from 0° to 360°. For each eligible tree, distance from plot center, azimuth (angle from true north), crown dominance class (dominant, co-dominant, understory), species, DBH, status (living or dead), and height (for dominant trees, measured with a clinometer) are recorded. When two or more trees share the same azimuth, measurements begin with the outermost tree and proceed inward. Trees that do not meet minimum DBH or height thresholds (red Xs on Figure) are skipped.

2.2.3 Remotely Piloted Aircraft Data Collection

A remotely piloted aircraft (RPA) was flown on August 11th and 12th 2022 at both Christie Bentham Wetland Trails and Ballyduff Trails, respectively. The aircraft was a DJI Matrice 600 Pro RPA which carried an integrated LiDAR sensor (a Riegl miniVUX-1UAV) and a Honeywell micro-electrical mechanical system inertial measurement unit (MEMS IMU-27). A Stonex 900 global navigation satellite system (GNSS) receiver was setup and running throughout the duration of each flight as a base station. Base station data were used with Novatel's NavLab (NovAtel Application Suite, n.d.) to correct the 3D spatial location of the RPA. Data were first processed based on RPA trajectory correction, IMU attitude adjustment, and colourized using Phoenix Lidar Systems LidarMill software (LiDARMill - Phoenix LiDAR Systems, n.d.).

For the Ballyduff Trails site, the RPA was flown at an average height of 88m above ground level (AGL) from the take-off position, collecting an average of 200 points/m^2 and average optical spatial resolution of 0.05 m derived from a flight pattern comprising 70% side and 80% forward overlap, flying at an average speed of 3.3 m/s with a single parallel flight line pattern, downward field of view (FOV) of 110 degrees, and scan pulse repetition rate of 100 KHz. To ensure accurate geolocation, 18 ground control points (GCPs) were dispersed throughout the property and measured with a Leica GS18 GNSS receiver. The same equipment and processing steps were used for flights at the Christie Bentham Wetland site with 8 GCPs. However, at Christie Bentham Wetland Trails, the RPA was flown at 4m/s at an average height of 60m AGL, which was possible due to a flatter terrain compared to Ballyduff. The point density acquired at Christie Bentham Wetland Trails had an average of 300 pts/m2 with an average optical image resolution of 0.05 m.

Point returns were processed using LiDARMill, which segmented the point cloud data into digital terrain, surface, and canopy height point clouds. Additional point return processing was conducted using a combination of CloudCompare (*CloudCompare - Open Source Project*, n.d.; Weidner et al., 2021), QGIS (Flenniken et al., 2020), and R (lidR, SF, tidyverse, raster, rgdal, viridisLite) (Atkins et al., 2022; Lai et al., 2023; Robinson & Hamann, 2010; Roussel et al., 2020) to remove noise and clip the processed point clouds to match the extents of the in-situ plots.

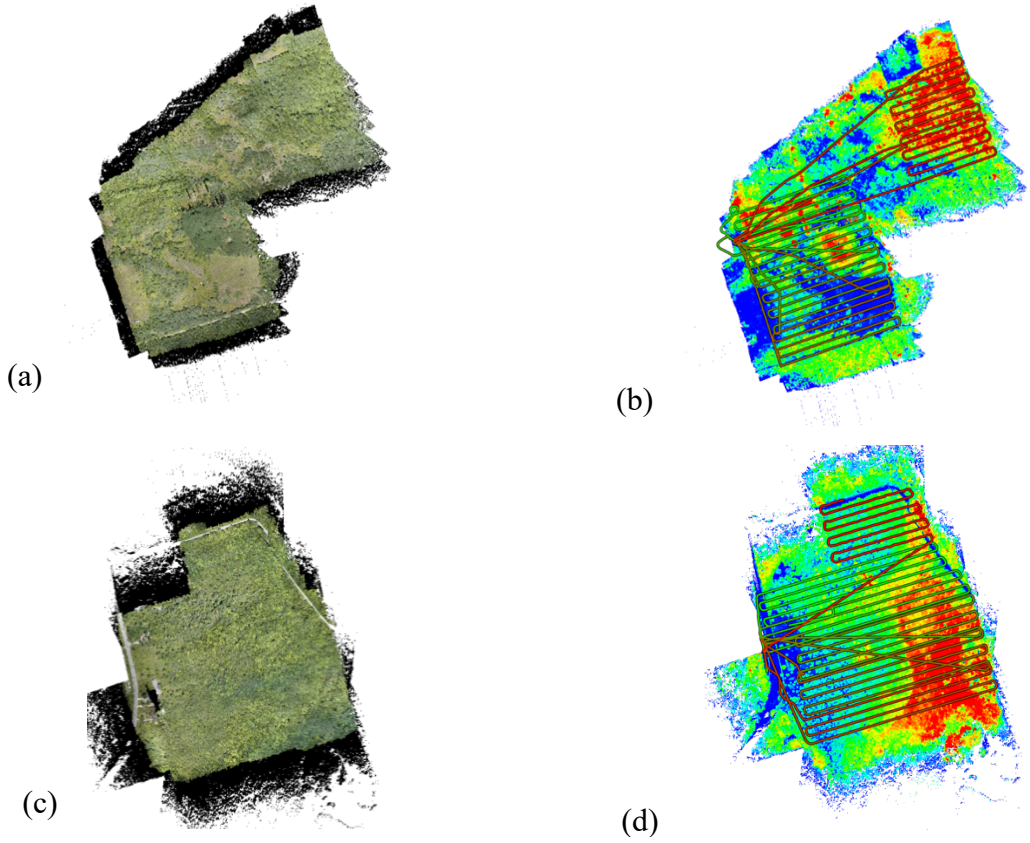


Figure 2.6. Plan views of RPA optical and LiDAR scans over two study areas: Ballyduff Trails (a, b) and Christie Bentham Wetland Trails (c, d). For Ballyduff Trails, (a) displays RGB visualization of the collected point cloud data, highlighting surface features in detail, while (b) illustrates the flight lines and the digital surface model (DSM) generated from the point cloud data, with elevation represented by a color gradient (red indicating higher elevations and blue indicating lower elevations). Similarly, for Christie Bentham Wetland Trails, (c) presents the RGB point cloud visualization, and (d) shows the flight lines and DSM using the same elevation color scheme, emphasizing the topographical variations across the wetlands.

Once the point-cloud data were cleaned and clipped to the study area (for both RPA and Aerial LiDAR), they were utilized to identify treetops by applying local maximum filters (e.g., Roussel et al., 2020). Additionally, the RGB images were processed with OpenSfM to generate 3D visualizations (e.g., Valluvan et al., 2023) enabling the identification of treetops. These processes were conducted using the lidR package in R (Figure 2.7, Roussel et al., 2020), which offers an extensive set of tools for processing LiDAR data acquired from various platforms, including drones. The lidR package can segment individual trees, compute a range of tree metrics (e.g., DBH, tree height), and use these data to estimate forest biomass and carbon.

```r
#locate treetops
treetops <- locate_trees(las_data, lmf(ws = ws))

# Calculate tree height
trees <- lastrees(las_data, treetops)

# Extract height from the metrics
trees$Height <- trees$tree_height

# Calculate DBH
trees <- trees %>%
  mutate(DBH = 1.63709725 * Height + (-4.2013447))

# Calculate biomass
trees$Biomass <- 0.0741 * (trees$DBH ^ 2.3875) + 0.0182 * (trees$DBH ^ 2.2181) + 0.0764 * (trees$DBH ^ 1.5861) + 0.0227 * (trees$DBH ^ 2.2797)
```

Figure 2.7. Example R code using the lidR package to (1) locate individual treetops within a LiDAR point cloud, (2) calculate tree height metrics, (3) apply an allometric equation to estimate DBH from tree height, and (4) compute biomass based on DBH using a set of exponent-based equations.

2.2.3 Aerial LiDAR

Mid-altitude pilot-on-board aircraft were used to acquire Aerial LiDAR for different areas of the province of Ontario. Aerial LiDAR data coinciding with the Ballyduff study area were acquired from the Digital Elevation Data to Support Flood Mapping (DEDSFM) Kawartha Lakes project supported by Natural Resources Canada (NRCan) under the Flood Hazard Identification and Mapping Program (FHIMP), which acquired LiDAR data from May 6th-10th, 2023. These Aerial LiDAR data were collected at a flight altitude 1650 m AGL with 40% side and forward overlap. The scan was done using a Riegl VQ1560ii-S sensor system flying at a speed of 160 knots with a single pass swath width of ~1730m, field of view (FOV) of 60 degrees, scan frequency of 320 Hz, scan pulse rate of 2100 Hz, and a pulse density of 11.5 points per square meter (PPSM), which yielded a spatial resolution of 0.5 m. The study had a non-vegetated RTK vertical accuracy (95%) of 7.2 cm / 173 points and a calculated horizontal accuracy (95%) of 30 cm.

Aerial LiDAR data coinciding with the Christie Bentham Wetland Trails study site were acquired from an OMAFRA (Ontario Ministry of Food, Agriculture and Rural Affairs) LiDAR Peterborough project, with acquisition occurring between November to December 2016 and April to May and October 2017 (Ministry of Natural Resources and Forestry, 2024). These Aerial LiDAR data were collected using a Leica ALS70-HP sensor system flying at a speed of 140 knots with a single pass swath width of 690m, FOV of 38 degrees, scan frequency of 313 Hz, scan pulse rate of 800 Hz, flightline spacing of 550m, and a pulse density of 8 PSM, which produced a spatial resolution of 0.5 m with ≤ 40% side and forward overlap. The study had a non-vegetated RTK vertical accuracy (95%) of 9.4 cm / 223 points and a calculated horizontal accuracy (95%) of 30 cm (Ministry of Natural Resources and Forestry, 2024).

The Aerial LiDAR point-cloud data were imported into CloudCompare (*CloudCompare - Open Source Project*, n.d.). Within CloudCompare, the individual data segments or tiles were merged, cleaned, and clipped to the study area boundary. Point cloud cleaning involved visually inspecting the point cloud

data and applying filters to eliminate noise or inaccuracies that could affect the reliability of subsequent analyses (Adams, 2000) including non-vegetative artifacts like birds, duplicate values, edge artifacts on the edges of surfaces and outliers.

2.2.4 Satellite LiDAR

Satellite-based LiDAR Forest metrics were collected using the GEDI module at a 90% level of confidence aboard the International Space Station. GEDI has several types of outputs (known as data packages) available that range from raw sensor data (level 1; L1) to processed AGB estimates (level 4; L4) that are released approximately 6 months after the initial data collection. Two specific products were acquired from the GEDI project for comparison against our in-situ and property parcel biomass and carbon assessments, which were the L2A and L4A. Level 2 products contain vertical height structure data with the L2A providing elevation and tree height metrics and L2B providing canopy cover and vertical tree profile metrics. Level 4 products contain biomass estimates with L4A providing footprint-level (25 m diameter) biomass estimates and L4B comprising gridded $1km^2$ biomass estimates (Dubayah et al., 2022; LP DAAC - GEDI Overview, n.d.). GEDI collects data using swaths of 8 beams spaced 60m apart at ground level with 25m diameter shots (LP DAAC - GEDI Overview, n.d.).

The GEDI shots were first used to identify locations for in-situ measurements, to ensure correspondence between the two. As part of the co-located site selection process, GEDI shots, taken between January 1st, 2019 and December 31st, 2022 were filtered to identify only those that were within 50 m of the parcel edge (to avoid edge effects). The result was 85 within the Ballyduff site and 50 within the Christie Bentham site (Figure 2.1 and 2.2). From these GEDI shot sites, in-situ sampling sites were chosen based partly on accessibility, distribution across the parcel, and adjacency. The second use of GEDI shots occurs in the estimation of forest biomass at the property parcel level (Section 2.3). At the property parcel level, all GEDI shots were used to estimate above-ground forest carbon.

2.3 Analysis

In our assessment of AGB, understanding the discrepancies between plot-level analysis and property-level analysis is crucial for understanding accurate and reliable estimations. While plot-level analysis provides detailed insights into localized biomass dynamics within specified areas, property parcel-level analysis offers a broader perspective of encompassing larger spatial scales. However, discrepancies between these two levels of analysis can arise due to various factors, including sampling methods, spatial heterogeneity, and scaling effects. In this study, we aim to investigate and compare AGB

estimations derived from plot-level and property parcel-level analyses, exploring the implication of these discrepancies for understanding biomass distribution and dynamics at different spatial scales.

2.3.1 Plot Level Analysis

The plot level analysis seeks to compare tree-biomass estimates at the plot level from four different scales of data acquisition: in-situ measurements, RPA LiDAR, aerial LiDAR, and satellite LiDAR data. The smaller area provides an understanding of accuracy and ability to capture variation in biomass estimates at a level of specificity that coincides with fixed-plot sampling and small areas of interest. Given the challenges associated with species identification from tree structural characteristics using LiDAR (Vaughn et al., 2012) and the additional sensor and analysis costs of using hyperspectral data (Michałowska & Rapiński, 2021) can limit its use, many forest biomass assessments, to date, use a generalized non-species specific allometric equation (e.g., Lambert et al., 2005). Generalized equations for North American forests (e.g., hardwood and softwood, spanning diverse ecological regions, Jenkins et al. 2003) have been widely adopted for national carbon stock assessments (e.g., Heath et al., 2011; Smith et al., 2007; US EPA, 2023) due to their balance of accuracy and applicability. These generalized allometric equations are designed to be applicable across a wide range of species and regions, providing a practical tool for large-scale biomass estimation that often yields very strong correlation between estimated and observed measurements (e.g., $R^2 = 0.90$, Xiang et al. 2016). Such an R^2 value indicates that 90% of the variation in observed biomass is captured by the model, highlighting the reliability and robustness of these equations for relating diameter-based metrics to actual biomass.

While species-specific equations may offer higher precision for individual species or localized studies, they require extensive field data and detailed knowledge of species characteristics, which may not be feasible for large-scale projects (Chave et al., 2005; Xiang et al., 2016). Estimates vary depending on how broadly one defines a “tree species,” but the Great Lakes–St. Lawrence forest region is often cited as having around 80+ native tree species (*The Tree Atlas | Ontario.Ca*, n.d.). As a transitional zone between the predominantly coniferous Boreal Forest to the north and the largely deciduous Carolinian Forest to the south, this region supports a mix of coniferous species, such as white pine (*Pinus strobus*), red pine (*Pinus resinosa*), and eastern hemlock (*Tsuga canadensis*), alongside various broadleaf species, including sugar maple (*Acer saccharum*), yellow birch (*Betula alleghaniensis*), and American beech (*Fagus grandifolia*). For our study to ensure spatial alignment of individual trees among the four scales of data acquisition would require the use of a global navigation satellite system (GNSS) receiver to locate each tree and corresponding in-situ measurement. Furthermore, the receiver would need to operate with sub meter accuracy (due to clustering, multi-stem). The high cost of GNSS receiver purchase, training, and

labour costs for use and analysis of sub-meter tree point locations, provide another justification for the use of a generalized non-species specific allometric equation. In absence of these additional tools, biomass was estimated for each individual tree from in-situ DBH measurements using species specific equations (Chojnacky et al., 2014; Lambert et al., 2005) and individual trees from LiDAR (i.e., aerial, RPA) using a generalized Canadian tree species allometric equation (Lambert et al., 2005). The estimated biomass for the entire plot was acquired by summing the biomass of all individual trees within the plot and reporting results as a density in tonnes per hectare.

The estimation of biomass at the plot level using LiDAR data was slightly different and acquired through the use of lidR package in R. Within lidR, LiDAR data were used to acquire canopy height measurements that were then used in a regression model to derive a DBH for each tree. Based on 23,567 tree metrics retrieved from the Tallo database (Jucker et al., 2022), after filtering to include only data within Canadian geographic extents, a linear regression analysis was performed on tree height and DBH values. The resulting equation predicts DBH from height values as follows:

$$D = 1.63709725 * H + (-4.2013447) \quad (2.8)$$

Equation 2.8 is a generalized linear regression equation for Canadian trees that calculates D (DBH in centimeters) using H (tree height in meters)

The derived DBH values were applied to the same generalized allometric equation applied to the in-situ DBH measurement to generate an estimate of individual tree biomass from the LiDAR data. Again, the individual-tree biomass estimates were summed to estimate biomass at the plot level.

Complementing the in-situ, RPA, and Aerial LiDAR, GEDI L4A data provided satellite-based biomass estimates as a density in tonnes per hectare, calculated by using derived tree height values within each 25m diameter shot and allometric equations stratified by region (all continents except Antarctica) and plant functional type (e.g., deciduous broad-leaf trees, evergreen broad-leaf trees, evergreen and deciduous needle-leaf trees, and combinations of woodlands, grasslands and shrubs) (Dubayah et al., 2020).

2.3.2 Property-Parcel Level Analysis

The same methodology for biomass calculation used at the plot level was also applied at the property-parcel level. However, since in-situ data collection and GEDI footprints only covered a small portion of the property parcel, in-situ and GEDI plot-level biomass estimates were used in an interpolation process to generate estimates of biomass where no measurements occurred for the Ballyduff site and for GEDI alone at the Christie Bentham Wetland Trails site (Figure 2.9). Given the greater computational overhead from Kriging compared to inverse-distance weighting interpolation (Meng et al.,

2013) and the difference in error between the two methods is small for small study areas (Kalivas et al., 2013; Zimmerman et al., 1999), an inverse-distance-weighting approach was used to estimate biomass in property-parcel locations void of in-situ measurements or GEDI shots similar to other forestry applications (e.g., Kalivas et al., 2013).

An assessment was conducted to determine whether GEDI shots located immediately outside property boundaries should be included in the biomass interpolation procedure. While GEDI data are generally valuable for measuring forest structure, observations revealed that many off-site shots occurred on farmland (e.g., near Ballyduff Trails) or within fragmented forests containing numerous gaps. Such conditions introduce edge effects and may not accurately represent forest interior characteristics. Consequently, these external points were excluded to maintain consistency and improve the validity of the interpolation results.

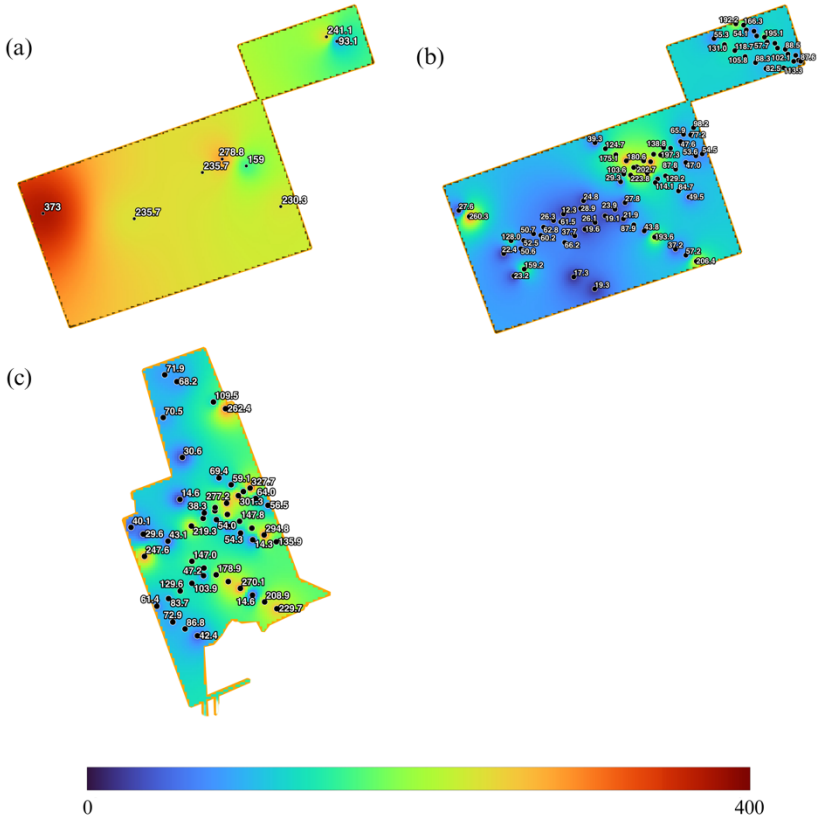


Figure 2.9. Interpolated views of in-situ and GEDI over two study areas: Ballyduff Trails (a, b) and Christie Bentham Wetland Trails (c, d). For Ballyduff Trails (a) displays an IDW interpolation using in-situ plot assessed biomass densities, (b) displays an IDW interpolation using GEDI based biomass densities. For Christie Bentham Wetland Trails (c) displays an IDW interpolation using GEDI based biomass densities.

Due to accessibility and personnel challenges (e.g., limited availability of data collectors), the Christie Bentham Wetland Trails site only contained three in-situ plots, which is insufficient for interpolation. Ideally, 4-10 plots per 10 hectares would offer a more representative sample of the entire forest. Therefore, the average of the three plot-level biomass estimates was multiplied by the total property parcel area to obtain a biomass estimate at that level. A similar approach was used for the RPA data, which did not cover the entire property parcel area for either study site (Figure 2.1, 2.2). Therefore, to generate an estimate for the entire study area, tree biomass estimates for the area covered by the RPA were summed and divided by the area covered to obtain biomass density in tonnes per hectare, which was then applied to locations that were not covered by the remotely piloted aircraft (RPA). Similar approaches are used with forest inventory data where results from sample plots conducted as part of the inventory are scaled up to forest stand or larger spatial units in a similar manner (McRoberts & Tomppo, 2007).

The only data providing complete coverage of the property parcels were those Aerial LiDAR data acquired by piloted mid-altitude aircraft (Section 2.2.3). For these data the same methodology used for obtaining a biomass estimate at the plot level was used to obtain an estimate at the property-parcel level.

3 Results

To assess the accuracy of various sensors applied at different altitudes above ground level in estimating biomass and carbon relative to in-situ measurements, we focused on key plot-level parameters: stem count, biomass in tonnes per hectare (T/ha), and tree type. The following results not only compare sensor-derived estimates with ground-truth data but also discuss the cost-benefit of data accuracy. This information aims to aid landowners, governments, and organizations in making informed decisions when faced with trade-offs among accuracy, spatial coverage, and project budget.

3.1 Plot-level analysis

To assess the accuracy of different scales of LiDAR acquisition relative to in-situ measurements, we compare the number of trees captured and then biomass density (t/ha) at the plot-level. In the absence of destructive sampling, tree count data provides one metric that is known with certainty whereas substantial error and uncertainty exists in most allometric equations (e.g., Mason et al., 2014; Vorster et al., 2020). Therefore, if a particular scale of data acquisition can more accurately capture the number of trees measured in-situ, it suggests that the scale has potential for tree-level biomass estimation.

Across the 10 plots sampled and two scales of LiDAR acquisition for which we could identify individual trees (RPA and Aerial), the RPA data produced a tree count that was more similar to the in-situ

tree count than Aerial data. The average tree-count accuracy was 69% using RPA data and 49% using Aerial data. Furthermore, the lowest accuracy of tree count for a plot was 35% and 19% for the RPA and Aerial data, respectively. While constraints in the number of plots covered by the RPA and our sample size limits our ability to state anything about statistical significance or confidence, when we compared across forest type, we found that stem count accuracy was lower for plots comprising primarily coniferous trees when Aerial LiDAR was used (Table 3.1). At the satellite level, an estimate of the number of trees within each GEDI shot is not provided in their Level 2 products and while it may be possible to derive tree density from full LiDAR waveforms, it is an output requiring further investigation and validation by the broader scientific community.

In our comparison of biomass estimates, relative to those based on our in-situ measurements, we incorporate GEDI, which provides these data as a direct output for public use (see Section 2.2.4). Comparing the biomass density (t/ha) across all data collection scales relative to our in-situ measurements (186.8 t/ha) reveals that GEDI produced the most similar result (187.2 t/ha, < 1% error) followed by the RPA (163.4 t/ha, 14% error) and Aerial LiDAR (131.0 t/ha, 56% error, Table 3.1). These densities differ substantially among each plot (Figure 3.1), whereby GEDI yielded the smallest amount of error on a percentage basis on 8 of 10 plots and Aerial LiDAR held the best results on two plots; however, RPA data were not acquired at those two plots. In 3 of 5 plots with RPA data, RPA plot biomass density values were substantially better than those estimated from Aerial LiDAR.

Table 3.1. Summary of in-situ plot level characteristics, stem counts, and biomass estimates as well as stem and biomass estimates from other data collection approaches (RPA, Aerial LiDAR, and GEDI). Results are provided only when coincident data were present.

	Plot #	Forest Type	Dominant Species	In-situ Average DBH (cm)	Tree Count			Biomass Density (t/ha)			
					In-situ	RPA	Aerial	In-situ	RPA	Aerial	GEDI
Baily Duff Trails	1	Deciduous	*Acer saccharum* (sugar maple)	24.2	16	N/A	12	373.0	N/A	327.5	260.3
	2	Deciduous	*Ostrya virginiana* (iron wood)	17.5	17	N/A	10	159.0	N/A	50.0	285.7
	3	Coniferous	*Pinus sylvestris* (Scott pine)	16.2	20	N/A	12	91.0	N/A	55.5	84.3
	4	Coniferous	*Thuja occidentalis L.* (eastern white cedar)	22.6	31	N/A	7	230.3	N/A	132.8	195.1
	6	Deciduous	*Populus grandidentata* Michx. (big tooth aspen)	19.8	17	6	11	235.7	64.9	110.3	223.8
	7	Mixed	*Ostrya virginiana* (American hophorn bean)	19.4	17	20	7	278.8	233.8	130.2	323.6
	8	Coniferous	*Thuja occidentalis* L. (eastern white cedar)	19.4	23	N/A	6	93.1	N/A	121.4	57.7
Christie Bentham	1	Mixed	*Ostrya virginiana* (iron wood)	16.2	15	12	6	96.6	41.2	11.0	71.9
	2	Mixed	*Ostrya virginiana* (iron wood)	13.5	30	16	11	84.2	47.0	39.8	68.2
	3	Deciduous	*Acer saccharum* (sugar maple)	19.5	18	11	11	226.7	430.3	331.1	301.3
			Average	18.8	20.4	13.0	9.3	186.8	163.4	131.0	187.2

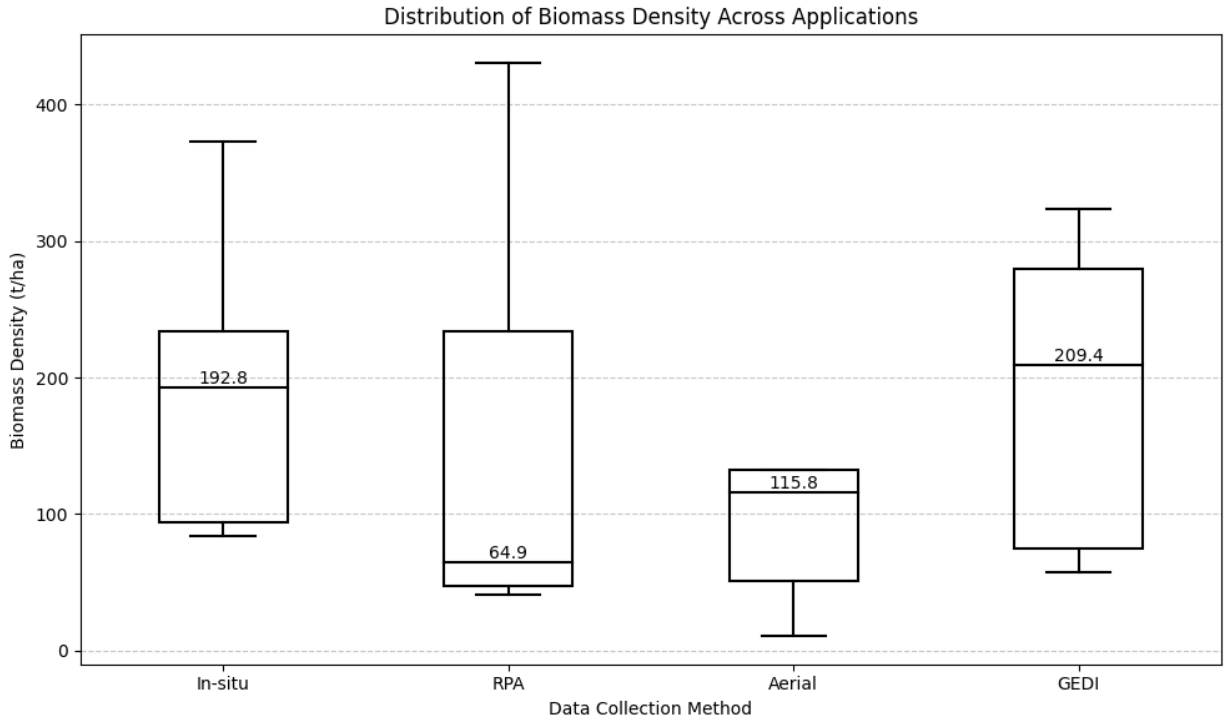


Figure 3.1: Box plots represent the distribution of biomass density measurements obtained through four different methods: In-situ, RPA, Aerial, and GEDI. Each box plot displays the median (black line), interquartile range, and variability of biomass density for each method.

No systematic over or under estimation of biomass was observed with any scale of LiDAR data collection (i.e., drone, aerial, satellite), which includes accounting for tree density and forest type. This suggests that more investigation of site information (e.g., topography), species, tree size and other potential factors driving differences in remotely sensed biomass estimation is required before statistical modelling (e.g., generalized additive modelling or machine learning) is pursued to better align remotely sensed observations with in-situ measurements.

It is worth noting, despite efforts to align the centroids of the GEDI shots with the plot centers of the collected in-situ data, two main sources of geolocation error exist. First, the GEDI system has a horizontal accuracy of approximately 10 meters (Dubayah et al., 2020). Second, the in-situ plot centers, determined using single-band frequency cellular devices exhibit a horizontal accuracy between 5 and 10 meters (Technologies, 2020). Consequently, the combined geolocation error between the reported GEDI centroid and the in-situ plot center can be as much as 20 meters. This geolocation error can affect biomass estimates in discontinuous forests, where vegetation structure and biomass can vary widely over short distances. However, in contiguous forests, like those used in this study, with relatively homogeneous

forest stands, the impact of geolocation discrepancies is reduced due to spatial autocorrelation. In such forests, similar forest characteristics are spatially correlated and consistent across the landscape minimizing the effect of positional inaccuracies on biomass estimates.

3.2 Property-Parcel analysis

Among our two study sites, Ballyduff was nearly completely forested (i.e., non-forested structures such as a wind turbine and maintained hiking trails were located within the property), and Christie Bentham was completely forested. Therefore, we assume that all properties comprise only forest and simple methods to scale results to the property parcel level are for comparative purposes and to showcase how plot level results differ when scaled to larger spatial extents.

Of the four scales of data acquisition (in situ, RPA, Aerial, and Satellite) only the Aerial LiDAR data, acquired by piloted aircraft, covered the entire area of the property parcels within our study. Both in-situ and GEDI-based forest metrics were used in an inverse distance weighting interpolation process to yield property parcel-level estimates. Since RPA LiDAR had substantial, but not full, spatial coverage of the property parcels, the average biomass for the area covered by the RPA was applied to the forested areas not covered by the RPA. A comparison across methods at the parcel scale is difficult given no single approach provides a benchmark for comparison as was provided by in-situ measurements at the plot level. Therefore, our parcel level results provide a quantification of the relative differences in tree-cover metrics and biomass estimates across these four data collection approaches.

As previously noted, the aerial coverage of our study was complete using mid-altitude piloted aircraft (i.e., aerial), which also had the lowest point density (i.e., 14 and 23 pts/m^2) of the LiDAR based approaches. In comparison, the RPA covered 42.5% and 67% percent of the Ballyduff and Christie Bentham study areas with average point cloud densities of 246 and 333 pts/m^2. Lastly, GEDI shots only covered 3.8 and 4.3% of the study areas at an average density of 22.4 pts/m^2. Satellite imagery are renowned for their extensive coverage over large spatial extents, however, our study found that aerial and drone-based LiDAR offered a superior coverage and higher spatial resolution for our specific area of interest compared to GEDI LiDAR shots.

The variation in tree density was substantial and spanned from 1070 to 417 trees per hectare across the two sites and four methods. In-situ extrapolation provided the highest estimated tree density (> 1000 trees/ha) at both sites, while the RPA yielded a similar estimate for Christie Bentham (970 trees/ha) and was slightly lower at Ballyduff (600 trees/ha). Aerial data yielded the lowest tree densities of 499 and 417 trees/ha, respectively, and individual tree data or their densities are not an output provided by or typically yielded from GEDI. These results are similar to observations at the plot level, which found that

the RPA yielded the closest tree counts to the in-situ counts, albeit they were systematically less. The higher density point clouds from the RPA are able to identify more trees (via local maximum values) than the aerial LiDAR data that have a point density that is an order of magnitude less. The RPA data yielded a lower average tree canopy height (10.1 m, and 11.6 m) than Aerial data (12.9 m and 17.2 m) at the Ballyduff Trails and Christie Bentham Wetland Trails sites, respectively. The GEDI data estimated the highest average tree canopy height of 16.3 and 20.9.

When comparing AGB estimates across LiDAR methodologies, property-parcel level values held greater consistency than plot level estimates. The estimated total parcel carbon across Ballyduff and Christie Bentham was lowest for the RPA (9994 t C, 4446 t C, respectively), higher for the Aerial data (14255 t C, 7060 t C), and highest for the in-situ and GEDI methods although the in-situ parcel carbon estimate was highest for Ballyduff (22450 t C) and GEDI was highest for the Christie Bentham parcel (8107 t C, Table 3.2). The RPA estimates were nearly half that derived from in-situ and GEDI despite its reasonable spatial coverage and representation of individual trees. When in-situ measurements are compared to an average of all LiDAR methods per study area, the average of all LiDAR methods was 22.34% and 21.80% lower for Ballyduff Trails and Christie Bentham Wetland Trails, respectively, than the in-situ measurements. RPA and aerial LiDAR offer extensive coverage but tend to underestimate biomass, which is likely due to missing smaller or understory trees.

Table 3.2 Comparison of parcel area, tree density, height, LiDAR point density, and aboveground biomass (AGB) estimates across In-situ, RPA, Aerial, and GEDI methods for Ballyduff and Christie Bentham study sites.

	Ballyduff				Christie Bentham			
	In-situ	RPA	Aerial	GEDI	In-situ	RPA	Aerial	GEDI
Parcel Area Assessed (ha)	0.14	45.8	107.6	4.1	0.06	37.2	55.5	2.4
Total Parcel Area (ha)	107.6	107.6	107.6	107.6	55.5	55.5	55.5	55.5
Average Parcel Tree Density (trees/ha)	1070.0	600.0	417.2	N/A	1045.0	970.0	499.0	N/A
Average Parcel Tree Height (m)	N/A	10.1	12.9	16.3	N/A	11.6	17.2	20.9
LiDAR Point Density (pts/m2)	N/A	246.0	14.0	22.4	N/A	333.0	23.0	22.4
Parcel AGB Density (t/ha)	208.7	92.9	132.5	200.2	135.8	80.2	127.3	146.2
Total Parcel AGB (t)	22450.0	9993.8	14254.7	21536.1	7533.7	4446.2	7060.2	8107.0

4 Discussion

Our multi-scale comparison of LiDAR data acquisition and subsequent tree biomass estimation contributes to remote sensing literature that primarily compares a single remote sensing approach to in-situ measurements, is sparce in the use of remotely piloted aircraft, and lacks study sites located within Canada. To situate our results, we conducted a literature search using Google Scholar with keywords “forest, carbon, multi-scale", between the years 2010-2024, which identified more than 24,000 returns. However, within the first 55 articles (sorted by relevance, Appendix A), 17 were excluded as unrelated (e.g., carbon composite materials, atmospheric emissions modeling) and 14 were excluded because they only looked at a single scale, one (e.g., Loran et al., 2016) or more sensors (e.g., Liu & Zhang, 2024) at a single scale (e.g., satellite). Of the remaining 24 articles, 23 discussed multi-scale comparisons of forest metrics, whereby 19 were limited to a single comparison (primarily satellite) with in-situ measurements while 3 articles involved two scales of comparison against in-situ measurements. Only two studies, combined in-situ, RPAS, aerial, and satellite LiDAR for aboveground biomass estimation, which was situated in Mozambique (Demol et al., 2024) and Australia (Kato et al., 2017).

Our multi-scale comparison of LiDAR derived carbon stock estimates is also unique in that among those 55 articles, only 30 included in-situ data, 25 included satellite data, 15 included aerial data, and only 11 included data collected using RPAS. Of the 15 articles using aerial data, only 9 included forest measurements and of the 11 papers using RPAS only four assessed forestry characteristics. The multi-scale comparisons involving RPAS only represent 5.5% of the reviewed literature and only two of those four used LiDAR (citations).

The result of our literature review demonstrates the dominance of in-situ and satellite data in forest inventory efforts and an underrepresentation of aerial and even more so RPAS-based forestry measurements. The scarcity of comprehensive, multi-scale LiDAR approaches is particularly pronounced in the context of Canadian forests. Canada’s forested landscapes, especially boreal ecosystems, differ substantially in structure, species composition, and disturbance regimes from many other regions (Brandt, 2009). These differences underscore the need for a more integrated and location-specific approach. By examining in-situ, RPAS, aerial, and satellite LiDAR data within a Canadian setting, this research addresses a critical gap in the literature and offers a benchmark for others to use or compare against. This benchmarking is of particular interest for those seeking to use RPAS, which have a great capacity to cover medium sized areas at point-cloud densities that are orders of magnitude greater than those acquired by aerial laser scanning and satellite, but typically less than those acquired by terrestrial laser scanning.

Our multi-scale comparison of LiDAR technology to estimate above-ground biomass of forest underestimated biomass compared to in-situ measurements. Specifically, RPA LiDAR, Aerial LiDAR,

and GEDI estimates averaged 136.42 t/ha, 121.67 t/ha, and 166.81 t/ha, respectively, against an in-situ average of 174.30 t/ha. These results corroborate the work of others who note that airborne LiDAR often underestimates biomass in low AGB plots (e.g., recently disturbed forests, boreal forests, or open woodland-savanna systems) and overestimates it in high AGB plots (e.g., forests with mature overstory; Ferraz et al. 2016). The underestimation of RPAS, aerial, and satellite based lidar relative to in-situ measurements is likely driven by the challenge of accurately detecting individual trees (Table 3.1) and subsequently tree density (Table 3.2), perhaps due in part to the lack of recognition of more and likely smaller trees observed between the canopies of larger trees which can be exacerbated in dense or structurally complex forests (Ferraz et al. 2016).

Despite our consistent underestimation of tree biomass at plot- and property levels, the LiDAR-based metrics were directionally aligned with the in-situ data and, similar to others, demonstrate the value and insight of forest structure, biomass, and when measured over time, dynamics, that can be achieved through the use of LiDAR (e.g., Coops et al., 2021; Kalivas et al., 2013; Nilsson, 1996; Popescu et al., 2003). Of particular interest for land managers is the capability of LiDAR technology to save time, labor, and cost relative to traditional methods, thereby reducing biases introduced by low sample counts inherent in in-situ assessments (Liang et al., 2018).

Of particular interest was the performance of GEDI and its close alignment with in-situ measurements, despite its lower point density relative to RPAS and location in space. It is likely that GEDI performed so well because the L4 product's reliance on robust modeling approaches trained on extensive datasets (Duncanson et al., 2022). The L4 product is the result of a simple Ordinary Least Squares (OLS) model with simulated Relative Height (RH) metrics and the accuracy of its results can vary considerably by region, often declining in areas with sparse training data or exceptionally high AGBD (Duncanson et al., 2022). Improved accuracy at more localized scales may be achievable with non-parametric models applied to raw GEDI data and as the volume and quality of training data increase. If similar modelling was conducted with aerial and RPAS LiDAR data then it is likely that improved accuracy would also be attainable.

It may also be possible to use interpolation with RPAS data as done was done with GEDI and similarly by others with GEDI (e.g., Kalivas et al. 2013). In this situation a sampling strategy would be required and used to either represent portions of large homogeneous forests or different conditions of forests that when tied to topography (e.g., slope and aspect) and other environmental conditions (e.g., hydrology) could yield greater biomass estimation accuracy.

4.1 Limitations

At the property-parcel scale, it is essential to acknowledge potential biases in our in-situ site selection. We specifically chose sites that were co-located with GEDI shots over forested areas. While this approach ensured a direct comparison between LiDAR and in-situ measurements within forested regions, it may have introduced biases related to site selection. For example, our focus on completely forested areas may have overestimated AGB at the parcel level, as our in-situ measurements did not account for non-forested regions such as pathways, wind turbines, rocky terrain, and clearings. When selecting GEDI shots across a parcel, we aimed for an equitable distribution of deciduous, coniferous, and mixed wood stands and tried to minimize edge effects by selecting points within 50 meters of a parcel boundary. Furthermore, for logistical efficiency, selected accessible points that were near each other, often opting for adjacent GEDI shots approximately 60 meters apart. While these choices facilitated the collection of more data, they introduced spatial clustering in our sampling.

In contrast to the in-situ and GEDI measurements, aerial and RPAS LiDAR-based applications considered not only forested areas but also non-forested regions to provide a more comprehensive assessment of AGB. This holistic approach can more accurately account for variation in the distribution of biomass across different land cover types, contributing to a more nuanced understanding of AGB dynamics. This underscores the importance of integrating multiple data sources to develop more accurate and holistic models for biomass estimation at the parcel level. By acknowledging the limitations and potential biases of our in-situ site selection, we emphasize the need for comprehensive sampling strategies that include a variety of land cover types. Integrating in-situ data with multiple scales of LiDAR data acquisition and other remote sensing data has the potential to improve the accuracy of biomass estimations, supporting more effective forestry management and construction of land-management policies.

The observed discrepancy or mismatch between LiDAR and in-situ collection may indicate that LiDAR values are not necessarily underestimated, but that in-situ values, when scaled to property level may overestimate biomass. This discrepancy could be attributed to the small sample size of in-situ measurements and the biases introduced from them. However, more multi-scale comparisons are required to gain a better understanding of the effects of scale on biomass estimation and more importantly is the need for a large set of destructive sampling data collected in coordination with multiple scales of LiDAR data acquisition.

4.2 Other sensors for biomass estimation

While our results provided a comparison of tree or forest biomass estimates across ground (in-situ), air (RPA, and aerial LiDAR), and satellite (via GEDI), there are a host of other sensors and

technologies that can be used to estimate biomass that were not included. For example, terrestrial laser scanning has been increasingly used to quantify tree and forest biomass (e.g., Bauwens et al., 2016; Calders et al., 2015; Liang et al., 2016). However, establishing absolute location information with a GNSS receiver or triangulation and registering common targets (sphere or planar) are time consuming and therefore constrain the spatial coverage of terrestrial laser scanning. In an effort to increase the speed of data collection, simultaneous localization and mapping (SLAM) technologies typically trade-off absolute location accuracy for the ability to cover an extensive ground area (e.g., Liang et al., 2015; Mokroš et al., 2021). Contemporary tools (e.g., Leica's BLK2GO, and Pheonix LiDAR's RECON-XT SLAM) can be used indoor and outdoor, cover substantially more area than TLS, and some SLAM tools are equipped to register point locations in open areas to spatially locate the point cloud while in the field. Perhaps even more versatile, although not yet proven to acquire the same levels of accuracy, mobile-phone apps that utilize novel flash LiDAR hardware (e.g., iPhone 12 Pro+) to acquire estimates of DBH (e.g., ForestScanner, Tatsumi et al. 2023) as well as 3D tree recreation using structure-from-motion (e.g., Valluvan et al., 2023). These on-the-ground developments have the potential to increase the speed of in-situ data collection and permit greater spatial coverage, but they cannot cover the same spatial area as remotely piloted aircraft (RPA) or mid-altitude pilot-on-board aircraft.

In addition to alternative terrestrial sensors are rapid improvements in sensors for mounting on RPA. As noted above, RPA point density is, on average, an order of magnitude denser (300 pts/m2) than Aerial LiDAR data (< 30pts/m2). At 300 pts/m2 we were unable to observe tree stem DBH when trees resided within a forest and required an additional statistical step to estimate DBH from tree height, which likely increased our plot and parcel level error. New sensors in 2024 from Riegl (e.g., Ultra 120) can be mounted on an RPA with a measurement rate of 2.4 million points per second and include forward and backward looking (10 degrees) capabilities, that have the capacity to produce point-cloud densities that are comparable to terrestrial laser scanning. However, the degree to which these points reach the tree stem remains to be determined.

Additional options are also possible among satellite-based sensors. For example, we attempted to incorporate carbon estimates from the advanced topographic laser altimeter system (ATLAS) on board the ice, cloud, and land elevation satellite 2 (ICESat-2). While the system is designed for high altitudes, it did cover our study area and has been useful in acquiring tree height information elsewhere (e.g., Neuenschwander & Magruder, 2019; Sothe et al., 2022; Xi et al., 2022). A comparison between height values derived from ICESat-2 with GEDI L2A and in-situ plot measurements revealed that the height estimates from ICESat-2 were reasonably close to those provided by GEDI and known in-situ data (Liu et al., 2021). However, the data density of ICESat-2 is much lower than GEDI and only a single average height estimate is acquired for each measurement swath (approximately 10 m by 120 m). Given the shape

and size of the ATLAS swath (1200 m^2) compared to a GEDI shot (491 m^2), it is likely that error from ATLAS estimates increase with landscape fragmentation, particularly in areas with substantial human infrastructure and open water where above-ground vegetation carbon is very low (which resides around our study parcels). These limitations underscore the importance of supplementary data, such as stem density, to enhance biomass estimations using ICESat-2 (Sothe et al., 2022) and why GEDI was used as a satellite-based approach for tree and forest biomass estimation.

5 Conclusions

Literature contains a variety of multi-scale analyses that quantify measurement accuracy and trade-offs among different sensors. However, the majority of that literature compares satellite-based sensors to in-situ measurements and very few pieces of literature truly look at multiple scales of LiDAR data acquisition, with even fewer including remotely piloted aircraft. As a contribution to the domain of remote sensing concerned with quantifying forest biomass and carbon, we presented a multi-scale analysis that included in-situ tree count and biomass estimates compared to those derived from LiDAR data acquired from remotely piloted aircraft (at a low altitude < 100 m above ground level), mid-altitude piloted aircraft, and the scale of satellites using GEDI mounted on the International Space Station. A comparison across these platforms at the plot and larger parcel level demonstrated that 1) remotely piloted aircraft yields the highest accuracy of tree reproduction relative to in-situ measurements, 2) the efforts to calibrate and validate GEDI results yielded the highest accuracy in carbon stock estimation relative to in-situ measurements, 3) at the parcel level, the greatest spatial coverage was obtained by mid-altitude aircraft, and 4) in most cases, the remote sensing approaches underestimated carbon stocks relative to in-situ measurements, including the average of all LiDAR methods yielding carbon stock estimates 21-22% lower than in-situ measurements, suggesting that small or below canopy trees are still likely poorly captured with the density of Aerial LiDAR points acquired and evaluated.

Despite the tendency of the evaluated multi-scale LiDAR sensors to yield lower carbon estimates relative to in-situ measurements, improvements to LiDAR continue and sensors like the Riegl Ultra 120 that are forward and backward looking, with nadir acquisition and very high pulse repetition rate (2.4 million points per second) suggest that aerial LiDAR data acquisition will soon approach the density acquired by terrestrial laser scanning (i.e., 10,000+ pts/m2). LiDAR's capability to capture tree and forest structural attributes and accurately mirror biomass trends across different areas in a forested environment, makes it invaluable for forest management and measurement, monitoring, and reporting and verification requirements. Furthermore, LiDAR-based AGB estimates will still require traditional forest inventories for calibration and validation, but they provide the capability to scale out forests assessments to very large

spatial extents and include areas where traditional ground-based forest inventories may be impractical, prohibitively expensive, or risk the safety of a field crew. Our comparison of LiDAR data acquisition at different scales for tree count and forest biomass estimation demonstrates the trade-offs between spatial coverage (e.g., mid-altitude aircraft) and improved accuracy (e.g., remotely piloted aircraft) against sample size and substantial calibration (e.g., GEDI). Ideally, our comparison offers insight to others seeking to quantify forest carbon and the relative influence their choice of platform may have on their results.

Additional efforts to systematically assess the effects of flight parameters (e.g., altitude, speed), sensor parameters (e.g., pulse repetition rate, beam divergence and footprint size, sensor angle), phenology (e.g., leaf on and leaf off conditions), and forest characteristics (e.g., tree density, DBH, species, and tree height) on tree count and carbon stock quantification is needed. Understanding the relative importance of some parameters over others could be incredibly valuable to forest carbon stock quantification efforts and provide supportive evidence for the development of a set of standard reporting variables that would further assist with comparative or meta-analyses.

Third Chapter: Advancements and Future Considerations

The precise quantification of forest biomass is crucial for understanding carbon dynamics, assessing biodiversity, and advancing Nature-based Solutions (NbS) across Canada (Seddon et al., 2020). As our understanding of environmental systems deepens, so too does the need for more accurate and reliable data on forest biomass, which plays a vital role in global carbon cycles and climate change mitigation efforts (Campbell et al., 2021). This chapter explores potential advancements in the methodologies currently employed for forest biomass estimation, examines future directions for these techniques, and considers their broader applications, particularly in urban environments. Enhancing these methodologies is essential for improving the accuracy and utility of biomass data, which in turn supports more informed decision-making in environmental management.

The focus of my research resided in leveraging advanced remote sensing technologies, specifically LiDAR-derived point cloud data, to quantify biomass and carbon storage with greater precision. Technologies like the Global Ecosystem Dynamics Investigation (GEDI) and the Ice, Cloud, and land Elevation Satellite-2 (ICESat-2) provide unique opportunities to assess biomass over large areas with unprecedented detail. However, the accuracy of these estimates can vary significantly depending on the specific LiDAR sensors employed, as each comes with its own set of limitations and specifications, such as point density and the altitude at which the data is collected. RADAR, another remote sensing technology, has also been used to estimate biomass. However, it faces challenges with signal penetration in dense forests (Quegan et al., 2019). In contrast, LiDAR's ability to capture the vertical structure of forests offers a more nuanced understanding of biomass distribution, particularly in areas with dense canopy cover where other technologies struggle to provide reliable data.

By addressing these variations and refining our methodologies, we can enhance the effectiveness of LiDAR as a tool for biomass estimation. Furthermore, the potential applications of these technologies extend beyond forested landscapes. This chapter explores advancements in methodologies and extended applications of LiDAR such as in urban forestry, where biomass estimation could contribute to urban forestry management and the development of green infrastructure. The chapter also discusses the transfer of knowledge and understanding from which currently remains primarily within the academic sphere to landowners and decision makers. Finally, this chapter will discuss the future advancements in technology that might allow for the increase in reliability and scalability of LiDAR-based forest biomass estimation. Doing so, this discussion underscores the importance of continuous innovation in remote sensing methodologies to meet the evolving needs of environmental management and to address the challenges posed by climate change.

Numerous studies have examined the effectiveness of LiDAR-based approaches for estimating above-ground biomass (e.g., Nilsson, 1996; Popescu et al., 2011; Sothe et al., 2022). However, few studies have compared multiple LiDAR methodologies within the same study area, as was conducted in the St. Williams Conservation Area by Robinson et al. (pers. comm). Such comparisons provide stakeholders with a clearer understanding of the level of detail needed for their projects, allowing them to balance the trade-offs between precision, cost, and time. Each LiDAR methodology, terrestrial, airborne (RPA and aerial), and satellite presents distinct advantages and limitations. Terrestrial LiDAR, often deployed in specific forest plots, provides unmatched spatial resolution, capable of measuring individual tree structures. However, it is constrained by its limited coverage and high operational costs. On the other hand, satellite-based systems like GEDI offer a broader perspective, covering large areas at a lower cost, but they may lack the fine-scale resolution needed for precise biomass estimation in heterogeneous landscapes. For instance, a project focused on monitoring biomass changes across several hundred hectares of forest over multiple years may not require in-situ or sub-centimeter accuracy. In these cases, aerial or satellite-based LiDAR data could be sufficient, offering a cost-effective alternative.

Future advancements in LiDAR technology and data processing techniques will likely further streamline these comparisons, providing even greater flexibility for stakeholders (e.g., Liu 2024). The role of LiDAR technology is constantly growing within the modern landscape from remote sensing, navigation, 3D modelling, to robotics (Raj et al., 2020), most noticeably for sectors like the automobile industry who leverage LiDAR to map their surroundings to estimate distances in a 3D view (S & A, 2023). As LiDAR technology continues to advance through multiple streams and/or industries, the accuracy and reliability of the data it produces becomes more prevalent as these improvements can be applied back to biomass estimation.

The improvement of LiDAR sensor and data processing has in the past and will in the future significantly enhance how it is able to capture and represent 3D vertical structures of forest data. The integration of machine learning and artificial intelligence into LiDAR data analysis could automate much of the decision-making process, allowing for more efficient selection of appropriate LiDAR methodologies for different project needs (Barbarella et al., 2021; Mohamed et al., 2022). The increasing availability of high-resolution, low-cost LiDAR data from multiple methods (e.g., satellite, RPAS) could democratise access to this technology, making it feasible for a wider range of projects and stakeholders (Abdollahnejad et al., 2019; Brach et al., 2023; Hu et al., 2021).

Additionally, advancements in multi-sensor integration, combining LiDAR with other remote sensing technologies such as hyperspectral imaging, RADAR, and optical imagery could enable more detailed ecological assessments (Goetz & Dubayah, 2011; Narine et al., 2009; Sothe et al., 2022). Furthermore, cloud-based processing allows data from LiDAR technology to be processed more

efficiently to create faster and more scalable data process pipelines while increasing collaboration. The increased scalability could be particularly beneficial for future conservation and land management projects, where understanding of multiple environmental factors, including biomass, vegetation health, and land use changes, will be critical for decision-making. By easing and improving the data collection and analysis phases, broader applications of the research can expand outside of the academic realm and better inform policy development. For example, improved biomass data could help guide restoration projects to target areas with the highest carbon storage potential (Cook-Patton et al., 2020).

One practical manifestation of these technological and methodological advancements can be seen in specialized software solutions developed to streamline LiDAR data analysis. For instance, DroneWatch a software offered by Korotu, provided as both a desktop application and cloud service, enables users to process and analyze LiDAR data with precision, focusing on detailed forest structure and biomass measurements at the individual tree level. The platform exemplifies how modern software can harness the power of drone-based LiDAR systems to collect data that is both scalable and precise, making it suitable for projects ranging from small conservation areas to large forested landscapes.

In comparison to other software like TreeMetrics, eCognition, and Fusion LiDAR, DroneWatch stands out for its tree-level precision. TreeMetrics focuses on commercial forest yields (e.g., Kaulen et al, 2023), eCognition excels in multispectral and area-based analysis (e.g., Machala & Zejdová, 2014), and Fusion LiDAR handles large-scale forest assessments but requires technical expertise (e.g., Mcgaughey, 2014). DroneWatch fills a niche by offering precise, user-friendly, individual tree analysis suited for small-scale or urban projects without need of expert level knowledge.

Similarly, while tools like Global Forest Watch, a platform developed by the World Resources Institute that uses near real-time satellite data to monitor forest cover changes globally, provide area-based, large-scale insights, DroneWatch complements these capabilities by offering detailed, ground-level metrics (Hansen et al., 2013; World Resources Institute, 2021). By integrating coarse-scale satellite surveillance with high-resolution, drone-based measurements, land managers can gain a more comprehensive understanding of forest carbon dynamics, from individual tree-level detail to broad landscape patterns.

Traditionally, models for assessing forest biomass (e.g., GEDI, GlobAllomeTree) use ground truth data for validating the accuracy and error rates, but like previously mentioned in-situ data is costly, time consuming, and labour intensive. These limitations such as restricted spatial coverage, logistical challenges and time constraints associated with in-situ models have prompted researchers to explore alternative data acquisition strategies (Anderson & Gaston, 2013). This shift has led to the increasing use of detailed RPAS data as a potential substitute for in-situ measurements in model validation processes (e.g., Anderson & Gaston, 2013; Turner et al., 2012). Although RPAS-based data acquisition may

introduce its own sources of uncertainty or error, it can still provide an acceptable level of accuracy depending on the specific analytic objectives. In some cases, the slight trade-off in precision compared to traditional ground truthing may be justified by the increased spatial coverage, operational efficiency, and cost-effectiveness that drone-derived information offers.

As technology continues to advance, drones equipped with advanced sensors (e.g., Riegl Ultra120[23] deploying a measurement rate of 2.4 million points per second) can collect data at granular levels, unveiling spatial variability that might be overlooked by in-situ measurements, which are often point specific and cover a very limited spatial extent. For instance, drones can survey extensive areas quickly and cover entire forested parcels while accounting for additional factors such as topographical changes and vegetation health depending on the type of sensor used (e.g., multi-spectral, Miles et al., 2003). By expanding spatial coverage and incorporating real-time changes across the property, models are validated against data that accurately reflects the dynamic nature of the study area.

Despite the numerous advantages, challenges and limitations exist in using drone data as a potential replacement for in-situ measurements. Data accuracy and precision can be affected by sensor limitations, calibration errors, and environmental factors such as weather conditions. Ensuring the quality and reliability of drone data necessitates rigorous calibration protocols and regular maintenance of equipment. Likewise, technical limitations, including limited battery life, payload capacity, and vulnerability to adverse weather conditions, can affect the duration and scope of data collection missions. Additionally, the large volumes of data generated by drones require substantial storage capacity and advanced data management solutions to process and analyze effectively.

In alignment with the aim of utilizing detailed drone data to potentially replace in-situ measurements for model validation, the GEDI mission has recently released a new data product, GEDI L4C. This product offers a comprehensive three-dimensional representation of canopy complexity by modeling 3D canopy structures from aerial LiDAR data and comparing them with over two billion high-quality, co-located GEDI observations (de Conto et al., 2024). This groundbreaking research demonstrates the effectiveness of employing detailed remotely sensed data as an alternative to traditional in-situ methods, highlighting limitations and sensitivities that are typically challenging to detect. Notably, the new model incorporates both vertical and horizontal variations in canopy structure, capturing 11% more variation than vertical variation alone derived from RH metrics (de Conto et al., 2024). This advancement underscores the potential of high-resolution remote sensing technologies in enhancing model validation processes by providing richer and more nuanced environmental data.

As these technologies continue to advance, they hold immense potential to significantly improve the accuracy and scalability of biomass estimation across diverse environments - from dense urban areas (Zhang & Shao, 2021) to expansive forest ecosystems. By leveraging high-resolution, remotely sensed

data to replace or supplement traditional in-situ measurements, we can enhance model validation processes, capturing complexities that were previously difficult to detect. This progression not only refines our ability to monitor and manage natural resources more effectively but also empowers us to make better-informed decisions in conservation and resource management. Ultimately, the integration of these innovative technologies marks a pivotal step toward more precise environmental modeling and sustainable stewardship of our planet's ecosystems.

Beyond the technical comparisons and accuracy assessments, the findings of this research hold broader significance for forest monitoring, policy, and modeling. Accurate, spatially explicit data on AGB are critical to forest governance and climate policy. Programs administered under the framework of the United Nations REDD+ initiative, for example, hinge on reliable carbon inventories to set baselines, track improvements, and guide financial incentives for forest protection and restoration (Angelsen, 2017; FAO, 2020). Such high-quality measurements feed directly into the reporting requirements set by accords like the Paris Agreement, informing Nationally Determined Contributions (NDCs) and enhancing the transparency and credibility of global efforts to mitigate climate change.

In this policy context, a few key concepts warrant attention: additionality, permanence, and leakage. Additionality speaks to whether observed emissions reductions or carbon gains would have occurred without a particular intervention; robust baseline AGB estimates can help confirm that credited improvements represent real progress rather than business-as-usual (BAU) scenarios. Permanence concerns the long-term stability of carbon stocks, an area where ongoing, high-resolution LiDAR monitoring can detect early signs of biomass loss and prompt corrective actions. Leakage, on the other hand, is the risk that reduced emissions in one area may trigger deforestation or degradation elsewhere. L By providing consistent, scalable, and accurate forest measurements, LiDAR technology can offer valuable insights into these issues, supporting robust and responsive forest monitoring efforts at various spatial scales.

Advances in LiDAR-based biomass estimation methods, combined with novel remote sensing technologies and improved analytical frameworks, represent a measured and evidence-driven response to the complexities of contemporary forest management. More accurate and scalable forest biomass data provide a firm scientific foundation for policies and practices aimed at carbon sequestration, habitat protection, and climate resilience (FAO, 2020; Seddon et al., 2020). By ensuring that decision-makers have access to spatially explicit, reliable information, these refinements help translate global agreements like the Paris Agreement and REDD+ commitments into effective, on-the-ground actions (Angelsen, 2017; UNFCCC, 2015). Rather than relying on assumptions or limited data sources, landowners, forest managers, and policymakers can draw on validated measurements of forest structure and carbon stocks to guide interventions that yield tangible ecological and socioeconomic benefits (Campbell et al., 2021). In

an era marked by rapid environmental change and pressing conservation challenges, the integration of LiDAR-derived metrics and related remote sensing innovations strengthens our capacity to safeguard forest ecosystems, inform policy choices, and ultimately enhance the resilience and sustainability of the landscapes we depend on.

References

Almeida, D. R. A., Broadbent, E. N., Zambrano, A. M. A., Wilkinson, B. E., Ferreira, M. E., Chazdon, R., Meli, P., Gorgens, E. B., Silva, C. A., Stark, S. C., Valbuena, R., Papa, D. A., & Brancalion, P. H. S. (2019). Monitoring the structure of forest restoration plantations with a drone-lidar system. *International Journal of Applied Earth Observation and Geoinformation*, *79*, 192–198. https://doi.org/10.1016/j.jag.2019.03.014

Anderson, K., & Gaston, K. J. (2013). Lightweight unmanned aerial vehicles will revolutionize spatial ecology. *Frontiers in Ecology and the Environment*, *11*(3), 138–146. https://doi.org/10.1890/120150

Angelsen, A. (2017). REDD+ as Result-based Aid: General Lessons and Bilateral Agreements of Norway. *Review of Development Economics*, *21*(2), 237–264. https://doi.org/10.1111/rode.12271

Araza, A., de Bruin, S., Herold, M., Quegan, S., Labriere, N., Rodriguez-Veiga, P., Avitabile, V., Santoro, M., Mitchard, E. T. A., Ryan, C. M., Phillips, O. L., Willcock, S., Verbeeck, H., Carreiras, J., Hein, L., Schelhaas, M.-J., Pacheco-Pascagaza, A. M., da Conceição Bispo, P., Laurin, G. V., … Lucas, R. (2022). A comprehensive framework for assessing the accuracy and uncertainty of global above-ground biomass maps. *Remote Sensing of Environment*, *272*, 112917. https://doi.org/10.1016/j.rse.2022.112917

Ballyduff Trails (McKim-Garsonnin)—Kawartha Land Trust. (2023, May 3). https://kawarthalandtrust.org/protected-properties/ballyduff-trails/

Bauwens, S., Bartholomeus, H., Calders, K., & Lejeune, P. (2016). Forest Inventory with Terrestrial LiDAR: A Comparison of Static and Hand-Held Mobile Laser Scanning. *Forests*, *7*(6), Article 6. https://doi.org/10.3390/f7060127

Beland, M., Parker, G., Sparrow, B., Harding, D., Chasmer, L., Phinn, S., Antonarakis, A., & Strahler, A. (2019). On promoting the use of lidar systems in forest ecosystem research. *Forest Ecology and Management*, *450*, 117484. https://doi.org/10.1016/j.foreco.2019.117484

Bonnor, G. M. (1972). Cost of a Small Forest Inventory. *Canadian Journal of Forest Research*, *2*(1), 45–48. https://doi.org/10.1139/x72-008

Brandeis, T. J., Delaney, M., Parresol, B. R., & Royer, L. (2006). Development of equations for predicting Puerto Rican subtropical dry forest biomass and volume. *Forest Ecology and Management*, *233*(1), 133–142. https://doi.org/10.1016/j.foreco.2006.06.012

Brandt, J. P. (2009). The extent of the North American boreal zone. *Environmental Reviews*, *17*(NA), 101–161. https://doi.org/10.1139/A09-004

Brown, S., Schroeder, P., & Birdsey, R. (1997). Aboveground biomass distribution of US eastern hardwood forests and the use of large trees as an indicator of forest development. *Forest Ecology and Management*, *96*(1), 37–47. https://doi.org/10.1016/S0378-1127(97)00044-3

Cabrera-Bosquet, L., Molero, G., Stellacci, A. N. N. A., Bort, J., Nogués, S., & Araus, J. (2011). NDVI as a potential tool for predicting biomass, plant nitrogen content and growth in wheat genotypes subjected to different water and nitrogen conditions. Cereal Research Communications, 39(1), 147-159.

Calders, K., Newnham, G., Burt, A., Murphy, S., Raumonen, P., Herold, M., Culvenor, D., Avitabile, V., Disney, M., Armston, J., & Kaasalainen, M. (2015). Nondestructive estimates of above-ground biomass using terrestrial laser scanning. *Methods in Ecology and Evolution*, *6*(2), 198–208. https://doi.org/10.1111/2041-210X.12301

Campbell, M. J., Dennison, P. E., Tune, J. W., Kannenberg, S. A., Kerr, K. L., Codding, B. F., & Anderegg, W. R. L. (2020). A multi-sensor, multi-scale approach to mapping tree mortality in woodland ecosystems. *Remote Sensing of Environment*, *245*, 111853. https://doi.org/10.1016/j.rse.2020.111853

Campbell, M. J., Dennison, P. E., Kerr, K. L., Brewer, S. C., & Anderegg, W. R. L. (2021). Scaled biomass estimation in woodland ecosystems: Testing the individual and combined capacities of satellite multispectral and lidar data. *Remote Sensing of Environment*, *262*, 112511. https://doi.org/10.1016/j.rse.2021.112511

Canada, N. R. (2008, February 4). *Species Identification & Typing*. Natural Resources Canada. https://www.nrcan.gc.ca/maps-tools-and-publications/satellite-imagery-and-air-photos/tutorial-fundamentals-remote-sensing/educational-resources-applications/forestry/species-identification-typing/9293

Carson, W. W., Andersen, H. E., Reutebuch, S. E., & McGaughey, R. J. (2004, May). LiDAR applications in forestry—An overview. In *ASPRS Annual Conference Proceedings* (p. 4).

Chausson, A., Turner, B., Seddon, D., Chabaneix, N., Girardin, C. A. J., Kapos, V., Key, I., Roe, D., Smith, A., Woroniecki, S., & Seddon, N. (2020). Mapping the effectiveness of nature-based solutions for climate change adaptation. *Global Change Biology*, *26*(11), 6134–6155. https://doi.org/10.1111/gcb.15310

Chave, J., Andalo, C., Brown, S., Cairns, M. A., Chambers, J. Q., Eamus, D., Fölster, H., Fromard, F., Higuchi, N., Kira, T., Lescure, J.-P., Nelson, B. W., Ogawa, H., Puig, H., Riéra, B., & Yamakura, T. (2005). Tree allometry and improved estimation of carbon stocks and balance in tropical forests. *Oecologia*, *145*(1), 87–99. https://doi.org/10.1007/s00442-005-0100-x

Chave, J., Davies, S. J., Phillips, O. L., Lewis, S. L., Sist, P., Schepaschenko, D., Armston, J., Baker, T. R., Coomes, D., Disney, M., Duncanson, L., Hérault, B., Labrière, N., Meyer, V., Réjou-Méchain, M., Scipal, K., & Saatchi, S. (2019). Ground Data are Essential for Biomass Remote Sensing Missions. *Surveys in Geophysics*, *40*(4), 863–880. https://doi.org/10.1007/s10712-019-09528-w

Chen, Y., & Zhu, X. (2013). An integrated GIS tool for automatic forest inventory estimates of Pinus radiata from LiDAR data. *GIScience & Remote Sensing*, *50*(6), 667–689. https://doi.org/10.1080/15481603.2013.866783

Chojnacky, D. C., Heath, L. S., & Jenkins, J. C. (2014). Updated generalized biomass equations for North American tree species. Forestry, 87(1), 129–151. https://doi.org/10.1093/forestry/cpt053

CloudCompare—Open Source project. (n.d.). Retrieved May 3, 2024, from https://www.danielgm.net/cc/

de Badereau, D., Roussel, H., & Tabbara, W. (2003). Radar Remote Sensing of Forest at Low Frequencies: A Two Dimensional Full Wave Approach. *Journal of Electromagnetic Waves and Applications*, *17*(6), 921–949. https://doi.org/10.1163/156939303322503510

De Cáceres, M., Martín-Alcón, S., González-Olabarria, J. R., & Coll, L. (2019). A general method for the classification of forest stands using species composition and vertical and horizontal structure. *Annals of Forest Science*, *76*(2), 40. https://doi.org/10.1007/s13595-019-0824-0

de Conto, T., Armston, J., & Dubayah, R. (2024). Characterizing the structural complexity of the Earth's forests with spaceborne lidar. *Nature Communications*, *15*(1), 8116. https://doi.org/10.1038/s41467-024-52468-2

Demol, M., Aguilar-Amuchastegui, N., Bernotaite, G., Disney, M., Duncanson, L., Elmendorp, E., Espejo, A., Furey, A., Hancock, S., Hansen, J., Horsley, H., Langa, S., Liang, M., Locke, A., Manjate, V., Mapanga, F., Omidvar, H., Parsons, A., Peneva-Reed, E., … Burt, A. (2024). Multi-scale lidar measurements suggest miombo woodlands contain substantially more carbon than thought. *Communications Earth & Environment*, *5*(1), 366. https://doi.org/10.1038/s43247-024-01448-x

Dubayah, R. O., Armston, J., Healey, S. P., Yang, Z., Patterson, P. L., Saarela, S., Stahl, G., Duncanson, L., & Kellner, J. R. (2022). *Global Ecosystem Dynamics Investigation (GEDI)GEDI L4B Gridded Aboveground Biomass Density, Version 2* [GTiff]. 0 MB. https://doi.org/10.3334/ORNLDAAC/2017

Dubayah, R. O., Armston, J., Kellner, J. R., Duncanson, L., Healey, S. P., Patterson, P. L., Hancock, S., Tang, H., Bruening, J., Hofton, M. A., Blair, J. B., & Luthcke, S. B. (2022). *Global Ecosystem Dynamics Investigation (GEDI)GEDI L4A Footprint Level Aboveground Biomass Density, Version 2.1* [HDF5]. 0 MB. https://doi.org/10.3334/ORNLDAAC/2056

Dubayah, R., Blair, J. B., Goetz, S., Fatoyinbo, L., Hansen, M., Healey, S., Hofton, M., Hurtt, G., Kellner, J., Luthcke, S., Armston, J., Tang, H., Duncanson, L., Hancock, S., Jantz, P., Marselis, S., Patterson, P. L., Qi, W., & Silva, C. (2020). The Global Ecosystem Dynamics Investigation: High-resolution laser ranging of the Earth's forests and topography. *Science of Remote Sensing*, *1*, 100002. https://doi.org/10.1016/j.srs.2020.100002

Duncanson, L., Kellner, J. R., Armston, J., Dubayah, R., Minor, D. M., Hancock, S., Healey, S. P., Patterson, P. L., Saarela, S., Marselis, S., Silva, C. E., Bruening, J., Goetz, S. J., Tang, H., Hofton, M., Blair, B., Luthcke, S., Fatoyinbo, L., Abernethy, K., … Zgraggen, C. (2022). Aboveground biomass density models for NASA's Global Ecosystem Dynamics Investigation (GEDI) lidar mission. *Remote Sensing of Environment*, *270*, 112845. https://doi.org/10.1016/j.rse.2021.112845

Falkowski, M. J., Wulder, M. A., White, J. C., & Gillis, M. D. (2009). Supporting large-area, sample-based forest inventories with very high spatial resolution satellite imagery. *Progress in Physical Geography: Earth and Environment*, *33*(3), 403–423. https://doi.org/10.1177/0309133309342643

FAO (2020). *Global Forest Resources Assessment 2020.* Rome, Italy.

Ferraz, A., Saatchi, S., Mallet, C., Jacquemoud, S., Gonçalves, G., Silva, C. A., Soares, P., Tomé, M., & Pereira, L. (2016). Airborne Lidar Estimation of Aboveground Forest Biomass in the Absence of Field Inventory. *Remote Sensing*, *8*(8), Article 8. https://doi.org/10.3390/rs8080653

Flade, L., Hopkinson, C., & Chasmer, L. (2020). Allometric Equations for Shrub and Short-Stature Tree Aboveground Biomass within Boreal Ecosystems of Northwestern Canada. *Forests*, *11*(11), Article 11. https://doi.org/10.3390/f11111207

Flenniken, M., Stuglik, S., & III, B. (2020). Quantum GIS (QGIS): An Introduction to a Free Alternative to More Costly GIS Platforms. *EDIS*, *2020*, 7. https://doi.org/10.32473/edis-fr428-2020

Gara, T., Sibanda, M., Shoko, C., Murwira, A., Ndaimani, H., & Hatendi, C. (2016). Estimating forest standing biomass in savanna woodlands as an indicator of forest productivity using the new generation WorldView-2 sensor. *Geocarto International*, 1–21. https://doi.org/10.1080/10106049.2016.1240717

Grabska, E., Hostert, P., Pflugmacher, D., & Ostapowicz, K. (2019). Forest Stand Species Mapping Using the Sentinel-2 Time Series. *Remote Sensing*, *11*(10), Article 10. https://doi.org/10.3390/rs11101197

GitHub—Mapillary/OpenSfM: Open source Structure-from-Motion pipeline. (n.d.). Retrieved September 28, 2024, from https://github.com/mapillary/OpenSfM?tab=readme-ov-file

Haara, A., & Haarala, M. (2002). Tree Species Classification using Semi-automatic Delineation of Trees on Aerial Images. *Scandinavian Journal of Forest Research*, *17*(6), 556–565. https://doi.org/10.1080/02827580260417215

Haghighatgou, N., Daniel, S., & Badard, T. (2022). A method for automatic identification of openings in buildings facades based on mobile LiDAR point clouds for assessing impacts of floodings. *International Journal of Applied Earth Observation and Geoinformation*, *108*, 102757. https://doi.org/10.1016/j.jag.2022.102757

Hansen, M. C., Potapov, P. V., Moore, R., Hancher, M., Turubanova, S. A., Tyukavina, A., Thau, D., Stehman, S. V., Goetz, S. J., Loveland, T. R., Kommareddy, A., Egorov, A., Chini, L., Justice, C. O., & Townshend, J. R. G. (2013). High-resolution global maps of 21st-century forest cover change. Science (New York, N.Y.), 342(6160), 850–853. https://doi.org/10.1126/science.1244693

Healey, S. P., Yang, Z., Gorelick, N., & Ilyushchenko, S. (2020). Highly Local Model Calibration with a New GEDI LiDAR Asset on Google Earth Engine Reduces Landsat Forest Height Signal Saturation. *Remote Sensing*, *12*(17), Article 17. https://doi.org/10.3390/rs12172840

Heath, L. S., Smith, J. E., Skog, K. E., Nowak, D. J., & Woodall, C. W. (2011). Managed Forest Carbon Estimates for the US Greenhouse Gas Inventory, 1990—2008. *Journal of Forestry*, *109*(3), 167–173. https://doi.org/10.1093/jof/109.3.167

Holopainena, M., & Talvitiea, M. (2004). *FOREST INVENTORY BY MEANS OF TREE-WISE 3 D-*

MEASUREMENTS OF LASER SCANNING DATA AND DIGITAL AERIAL PHOTOGRAPHS. https://www.semanticscholar.org/paper/FOREST-INVENTORY-BY-MEANS-OF-TREE-WISE-3-OF-LASER-Holopainena-Talvitiea/c004335e608f9c85e53d3c705a745d96da3dc84d

Hu, T., Sun, X., Su, Y., Guan, H., Sun, Q., Kelly, M., & Guo, Q. (2021). Development and Performance Evaluation of a Very Low-Cost UAV-Lidar System for Forestry Applications. *Remote Sensing*, *13*(1), Article 1. https://doi.org/10.3390/rs13010077

Jucker, T., Fischer, F., Chave, J., Coomes, D., Caspersen, J., Ali, A., Loubota Panzou, G. J., Feldpausch, T., Falster, D., Usoltsev, V., Adu-Bredu, S., Alves, L., Aminpour, M., Angoboy, I., Anten, N., Antin, C., Askari, Y., Avilés, R. M., Ayyappan, N., … Zavala, M. (2022). *Tallo database* [dataset]. Zenodo. https://doi.org/10.5281/zenodo.6637599

Kaulen, A., Stopfer, L., Lippert, K., & Purfürst, T. (2023). Systematics of forestry technology for tracing the timber supply chain. *Forests*, *14*(9), 1718.

Kalivas, Dionissios. P., KOLLIAS, Vassiliki. J., & APOSTOLIDIS, Ektoras. H. (2013). Evaluation of three spatial interpolation methods to estimate forest volume in the municipal forest of the Greek island Skyros. *Geo-Spatial Information Science*, *16*(2), 100–112. https://doi.org/10.1080/10095020.2013.766398

Kumar, L., & Mutanga, O. (2017). Remote Sensing of Above-Ground Biomass. *Remote Sensing*, *9*(9), Article 9. https://doi.org/10.3390/rs9090935

Lambert, M.-C., Ung, C.-H., & Raulier, F. (2005). Canadian national tree aboveground biomass equations. *Canadian Journal of Forest Research*, *35*(8), 1996–2018. https://doi.org/10.1139/x05-112

Larjavaara, M., & Muller-Landau, H. C. (2013). Measuring tree height: A quantitative comparison of two common field methods in a moist tropical forest. *Methods in Ecology and Evolution*, *4*(9), 793–801. https://doi.org/10.1111/2041-210X.12071

Li, X., Wu, J., Lu, S., Li, D., & Lu, D. (2024). Integration of Handheld and Airborne Lidar Data for Dicranopteris Dichotoma Biomass Estimation in a Subtropical Region of Fujian Province, China. *Remote Sensing*, *16*(12), Article 12. https://doi.org/10.3390/rs16122088

Li, Y., Andersen, H.-E., & McGaughey, R. (2008). A Comparison of Statistical Methods for Estimating Forest Biomass from Light Detection and Ranging Data. *Western Journal of Applied Forestry*, *23*(4), 223–231. https://doi.org/10.1093/wjaf/23.4.223

Li, Y., Li, C., Li, M., & Liu, Z. (2019). Influence of Variable Selection and Forest Type on Forest Aboveground Biomass Estimation Using Machine Learning Algorithms. *Forests*, *10*(12), Article 12. https://doi.org/10.3390/f10121073

Liang, X., Kankare, V., Hyyppä, J., Wang, Y., Kukko, A., Haggrén, H., Yu, X., Kaartinen, H., Jaakkola, A., Guan, F., Holopainen, M., & Vastaranta, M. (2016). Terrestrial laser scanning in forest inventories. *ISPRS Journal of Photogrammetry and Remote Sensing*, *115*, 63–77. https://doi.org/10.1016/j.isprsjprs.2016.01.006

Liang, X., Kukko, A., Hyyppä, J., Lehtomäki, M., Pyörälä, J., Yu, X., Kaartinen, H., Jaakkola, A., & Wang, Y. (2018). In-situ measurements from mobile platforms: An emerging approach to address the old challenges associated with forest inventories. *ISPRS Journal of Photogrammetry and Remote Sensing*, *143*, 97–107. https://doi.org/10.1016/j.isprsjprs.2018.04.019

Liang, X., Wang, Y., Jaakkola, A., Kukko, A., Kaartinen, H., Hyyppä, J., Honkavaara, E., & Liu, J. (2015). Forest Data Collection Using Terrestrial Image-Based Point Clouds From a Handheld Camera Compared to Terrestrial and Personal Laser Scanning. *IEEE Transactions on Geoscience and Remote Sensing*, *53*(9), 5117–5132. IEEE Transactions on Geoscience and Remote Sensing. https://doi.org/10.1109/TGRS.2015.2417316

LiDARMill—Phoenix LiDAR Systems. (n.d.). Retrieved July 13, 2024, from https://phoenixlidar.com/category/product/lidarmill/

Liu, A., Cheng, X., & Chen, Z. (2021). Performance evaluation of GEDI and ICESat-2 laser altimeter data for terrain and canopy height retrievals. *Remote Sensing of Environment*, *264*, 112571. https://doi.org/10.1016/j.rse.2021.112571

Liu, C. (2024). *Assessing Tree Carbon Estimates from Remotely Piloted Aircraft-Based LiDAR: A Comparison of Quantitative Structural Models and Allometric Scaling with In-Situ DBH Measurements*. https://hdl.handle.net/10012/21066

LP DAAC - GEDI Overview. (n.d.). Retrieved December 2, 2022, from https://lpdaac.usgs.gov/data/get--data/collection-overview/missions/gedi-overview/

Luoma, V., Saarinen, N., Wulder, M. A., White, J. C., Vastaranta, M., Holopainen, M., & Hyyppä, J. (2017). Assessing Precision in Conventional Field Measurements of Individual Tree Attributes. *Forests*, *8*(2), Article 2. https://doi.org/10.3390/f8020038

Machala, M., & Zejdová, L. (2014). Forest Mapping Through Object-based Image Analysis of Multispectral and LiDAR Aerial Data. *European Journal of Remote Sensing*, *47*(1), 117–131. https://doi.org/10.5721/EuJRS20144708

Mcgaughey, R. (2014). FUSION/LDV: Software for LiDAR data analysis and visualization - V3.10. *USDA Forest Service*.

Martin, A. J. F. (2022). Accuracy and Precision in Urban Forestry Tools for Estimating Total Tree Height. *Arboriculture & Urban Forestry (AUF)*, *48*(6), 319–332. https://doi.org/10.48044/jauf.2022.024

Mason, N. W. H., Beets, P. N., Payton, I., Burrows, L., Holdaway, R. J., & Carswell, F. E. (2014). Individual-Based Allometric Equations Accurately Measure Carbon Storage and Sequestration in Shrublands. *Forests*, *5*(2), Article 2. https://doi.org/10.3390/f5020309

McRoberts, R. E., & Tomppo, E. O. (2007). Remote sensing support for national forest inventories. *Remote Sensing of Environment*, *110*(4), 412–419. https://doi.org/10.1016/j.rse.2006.09.034

Meinen, B. U., & Robinson, D. T. (2020). Streambank topography: An accuracy assessment of UAV-based and traditional 3D reconstructions. *International Journal of Remote Sensing*, *41*(1), 1–18. https://doi.org/10.1080/01431161.2019.1597294

Meinen, B. U., & Robinson, D. T. (2021). Agricultural erosion modelling: Evaluating USLE and WEPP field-scale erosion estimates using UAV time-series data. *Environmental Modelling & Software*, *137*, 104962. https://doi.org/10.1016/j.envsoft.2021.104962

Meng, Q., Liu, Z., & Borders, B. E. (2013). Assessment of regression kriging for spatial interpolation – comparisons of seven GIS interpolation methods. *Cartography and Geographic Information Science*, *40*(1), 28–39. https://doi.org/10.1080/15230406.2013.762138

Michałowska, M., & Rapiński, J. (2021). A Review of Tree Species Classification Based on Airborne LiDAR Data and Applied Classifiers. *Remote Sensing*, *13*(3), Article 3. https://doi.org/10.3390/rs13030353

Miles, V. V., Bobylev*, L. P., Maximov, S. V., Johannessen, O. M., & Pitulko, V. M. (2003). An approach for assessing boreal forest conditions based on combined use of satellite SAR and multi-spectral data. *International Journal of Remote Sensing*, *24*(22), 4447–4466. https://doi.org/10.1080/0143116031000070436

Mohareb, E., & Kennedy, C. (2012). Gross Direct and Embodied Carbon Sinks for Urban Inventories. *Journal of Industrial Ecology*, *16*(3), 302–316. https://doi.org/10.1111/j.1530-9290.2011.00445.x

Mokroš, M., Mikita, T., Singh, A., Tomaštík, J., Chudá, J., Wężyk, P., Kuželka, K., Surový, P., Klimánek, M., Zięba-Kulawik, K., Bobrowski, R., & Liang, X. (2021). Novel low-cost mobile mapping systems for forest inventories as terrestrial laser scanning alternatives. *International Journal of Applied Earth Observation and Geoinformation*, *104*, 102512. https://doi.org/10.1016/j.jag.2021.102512

Mora, B., Wulder, M. A., & White, J. C. (2010). Identifying leading species using tree crown metrics derived from very high spatial resolution imagery in a boreal forest environment. *Canadian Journal of Remote Sensing*, *36*(4), 332–344. https://doi.org/10.5589/m10-052

Neuenschwander, A. L., & Magruder, L. A. (2019). Canopy and Terrain Height Retrievals with ICESat-2: A First Look. *Remote Sensing*, *11*(14), Article 14. https://doi.org/10.3390/rs11141721

NovAtel Application Suite. (n.d.). Retrieved July 13, 2024, from https://docs.novatel.com/Tools/Content/ToolsSuite/Overview.htm

Novo-Fernández, A., Barrio-Anta, M., Recondo, C., Cámara-Obregón, A., & López-Sánchez, C. A. (2019). Integration of National Forest Inventory and Nationwide Airborne Laser Scanning Data to Improve Forest Yield Predictions in North-Western Spain. *Remote Sensing*, *11*(14), Article 14. https://doi.org/10.3390/rs11141693

Paul, K. I., Roxburgh, S. H., England, J. R., Ritson, P., Hobbs, T., Brooksbank, K., John Raison, R., Larmour, J. S., Murphy, S., Norris, J., Neumann, C., Lewis, T., Jonson, J., Carter, J. L., McArthur, G., Barton, C., & Rose, B. (2013). Development and testing of allometric equations

for estimating above-ground biomass of mixed-species environmental plantings. *Forest Ecology and Management*, *310*, 483–494. https://doi.org/10.1016/j.foreco.2013.08.054

Peinecke, N., Lueken, T., & Korn, B. R. (2008). Lidar simulation using graphics hardware acceleration. *2008 IEEE/AIAA 27th Digital Avionics Systems Conference*, 4.D.4-1-4.D.4-8. https://doi.org/10.1109/DASC.2008.4702838

Petersson, H., Holm, S., Ståhl, G., Alger, D., Fridman, J., Lehtonen, A., Lundström, A., & Mäkipää, R. (2012). Individual tree biomass equations or biomass expansion factors for assessment of carbon stock changes in living biomass – A comparative study. *Forest Ecology and Management*, *270*, 78–84. https://doi.org/10.1016/j.foreco.2012.01.004

Pettorelli, N., Graham, N. A. J., Seddon, N., Maria da Cunha Bustamante, M., Lowton, M. J., Sutherland, W. J., Koldewey, H. J., Prentice, H. C., & Barlow, J. (2021). Time to integrate global climate change and biodiversity science-policy agendas. *Journal of Applied Ecology*, *58*(11), 2384–2393. https://doi.org/10.1111/1365-2664.13985

Provincial Mapping, Mapping and Information Resources Branch, Corporate Management and Information Division, Ministry of Natural Resources and Forestry. (2024, January 17). *User guide for Ontario digital surface model (Lidar-derived): Land Information Ontario dataset*.

Quegan, S., Le Toan, T., Chave, J., Dall, J., Exbrayat, J.-F., Minh, D. H. T., Lomas, M., D'Alessandro, M. M., Paillou, P., Papathanassiou, K., Rocca, F., Saatchi, S., Scipal, K., Shugart, H., Smallman, T. L., Soja, M. J., Tebaldini, S., Ulander, L., Villard, L., & Williams, M. (2019). The European Space Agency BIOMASS mission: Measuring forest above-ground biomass from space. *Remote Sensing of Environment*, *227*, 44–60. https://doi.org/10.1016/j.rse.2019.03.032

Roberts, D., Boon, R., Diederichs, N., Douwes, E., Govender, N., Mcinnes, A., Mclean, C., O'Donoghue, S., & Spires, M. (2012). Exploring ecosystem-based adaptation in Durban, South Africa: "Learning-by-doing" at the local government coal face. *Environment and Urbanization*, *24*(1), 167–195. https://doi.org/10.1177/0956247811431412

Roussel, J.-R., Auty, D., Coops, N. C., Tompalski, P., Goodbody, T. R. H., Meador, A. S., Bourdon, J.-F., de Boissieu, F., & Achim, A. (2020). lidR: An R package for analysis of Airborne Laser Scanning (ALS) data. *Remote Sensing of Environment*, *251*, 112061. https://doi.org/10.1016/j.rse.2020.112061

Seddon, N., Chausson, A., Berry, P., Girardin, C. A. J., Smith, A., & Turner, B. (2020). Understanding the value and limits of nature-based solutions to climate change and other global challenges. *Philosophical Transactions of the Royal Society B: Biological Sciences*, *375*(1794), 20190120. https://doi.org/10.1098/rstb.2019.0120

Seddon, N., Smith, A., Smith, P., Key, I., Chausson, A., Girardin, C., House, J., Srivastava, S., & Turner, B. (2021). Getting the message right on nature-based solutions to climate change. *Global Change Biology*, *27*(8), 1518–1546. https://doi.org/10.1111/gcb.15513

Sidik, S. M. (2022, April 6). *Scientists Fight to Keep Lidar on the Space Station*. Eos. http://eos.org/articles/scientists-fight-to-keep-lidar-on-the-space-station

Smith, J. E., Heath, L. S., & Nichols, M. C. (2007). US forest carbon calculation tool: Forest-land carbon

stocks and net annual stock change. *Revised. Gen. Tech. Rep. NRS-13. Newtown Square, PA: U.S. Department of Agriculture, Forest Service, Northern Research Station. 34 p. [DVD-ROM].*, *13*. https://doi.org/10.2737/NRS-GTR-13

Sothe, C., Gonsamo, A., Arabian, J., Kurz, W. A., Finkelstein, S. A., & Snider, J. (2022). Large Soil Carbon Storage in Terrestrial Ecosystems of Canada. *Global Biogeochemical Cycles*, *36*(2), e2021GB007213. https://doi.org/10.1029/2021GB007213

Sothe, C., Gonsamo, A., Lourenço, R. B., Kurz, W. A., & Snider, J. (2022). Spatially Continuous Mapping of Forest Canopy Height in Canada by Combining GEDI and ICESat-2 with PALSAR and Sentinel. *Remote Sensing*, *14*(20), Article 20. https://doi.org/10.3390/rs14205158

Spinelli, R., Magagnotti, N., Pari, L., & Soucy, M. (2016). Comparing Tree Selection as Performed by Different Professional Figures. *Forest Science*, *62*(2), 213–219. https://doi.org/10.5849/forsci.15-062

Stovall, A. E. L., Anderson-Teixeira, K. J., & Shugart, H. H. (2018). Assessing terrestrial laser scanning for developing non-destructive biomass allometry. *Forest Ecology and Management*, *427*, 217–229. https://doi.org/10.1016/j.foreco.2018.06.004

STP-H7 and H8 Scientific Payloads Successfully Installed, Collecting Data on the ISS. (n.d.). Space Systems Command. Retrieved February 1, 2023, from https://www.ssc.spaceforce.mil/Newsroom/Article-Display/Article/2904427/https%3A%2F%2Fwww.ssc.spaceforce.mil%2FNewsroom%2FArticle-Display%2FArticle%2F2904427%2Fstp-h7-and-h8-scientific-payloads-successfully-installed-collecting-data-on-the

Stuart, J. D. (1984). Hazard rating of lodgepole pine stands to mountain pine beetle outbreaks in southcentral Oregon. *Canadian Journal of Forest Research*, *14*(5), 666–671. https://doi.org/10.1139/x84-120

Tatsumi, S., Yamaguchi, K., & Furuya, N. (2023). ForestScanner: A mobile application for measuring and mapping trees with LiDAR-equipped iPhone and iPad. *Methods in Ecology and Evolution*, *14*(7), 1603–1609. https://doi.org/10.1111/2041-210X.13900

Technologies, !important Safety. (2020, June 11). We Tested Mobile GPS/GNSS Accuracy and Found Some Surprising Results. *Medium*. https://medium.com/@importanttech/we-tested-mobile-gps-gnss-accuracy-and-found-some-surprising-results-b9ec35873e2e

The Tree Atlas | ontario.ca. (n.d.). Retrieved December 24, 2024, from http://www.ontario.ca/page/tree-atlas

Turner, D., Lucieer, A., & Watson, C. (2012). An Automated Technique for Generating Georectified Mosaics from Ultra-High Resolution Unmanned Aerial Vehicle (UAV) Imagery, Based on Structure from Motion (SfM) Point Clouds. *Remote Sensing*, *4*(5), Article 5. https://doi.org/10.3390/rs4051392

US EPA, O. (2015, August 28). *Greenhouse Gas Equivalencies Calculator* [Data and Tools]. https://www.epa.gov/energy/greenhouse-gas-equivalencies-calculator

US EPA, O. (2023, February 1). *Inventory of U.S. Greenhouse Gas Emissions and Sinks: 1990-2021* [Reports and Assessments]. https://www.epa.gov/ghgemissions/inventory-us-greenhouse-gas-emissions-and-sinks-1990-2021

Vaglio Laurin, G., Chen, Q., Lindsell, J. A., Coomes, D. A., Frate, F. D., Guerriero, L., Pirotti, F., & Valentini, R. (2014). Above ground biomass estimation in an African tropical forest with lidar and hyperspectral data. *ISPRS Journal of Photogrammetry and Remote Sensing*, *89*, 49–58. https://doi.org/10.1016/j.isprsjprs.2014.01.001

Valluvan, A. B., Raj, R., Pingale, R., & Jagarlapudi, A. (2023). Canopy height estimation using drone-based RGB images. *Smart Agricultural Technology*, *4*, 100145. https://doi.org/10.1016/j.atech.2022.100145

Vaughn, N. R., Moskal, L. M., & Turnblom, E. C. (2012). Tree Species Detection Accuracies Using Discrete Point Lidar and Airborne Waveform Lidar. *Remote Sensing*, *4*(2), Article 2. https://doi.org/10.3390/rs4020377

Vegetation Sampling Protocol (VSP). (n.d.). Retrieved April 16, 2024, from http://forests-settled-urban-landscapes.org/VSP/

Vorster, A. G., Evangelista, P. H., Stovall, A. E. L., & Ex, S. (2020). Variability and uncertainty in forest biomass estimates from the tree to landscape scale: The role of allometric equations. *Carbon Balance and Management*, *15*(1), 8. https://doi.org/10.1186/s13021-020-00143-6

Wang, J., Sammis, T. W., Gutschick, V. P., Gebremichael, M., Dennis, S. O., & Harrison, R. E. (2010). Review of Satellite Remote Sensing Use in Forest Health Studies~!2010-01-27~!2010-04-05~!2010-06-29~! *The Open Geography Journal*, *3*(1), 28–42. https://doi.org/10.2174/1874923201003010028

Weng, Q. (2011). *Advances in Environmental Remote Sensing: Sensors, Algorithms, and Applications*. CRC Press.

What is Random Forest? | IBM. (n.d.). Retrieved July 5, 2023, from https://www.ibm.com/topics/random-forest

Woodall, C. W., Amacher, M. C., Bechtold, W. A., Coulston, J. W., Jovan, S., Perry, C. H., Randolph, K. C., Schulz, B. K., Smith, G. C., Tkacz, B., & Will-Wolf, S. (2011). Status and future of the forest health indicators program of the USA. *Environmental Monitoring and Assessment*, *177*(1–4), 419–436. https://doi.org/10.1007/s10661-010-1644-8

Woods, J. O., & Christian, J. A. (2016). Lidar-based relative navigation with respect to non-cooperative objects. *Acta Astronautica*, *126*, 298–311. https://doi.org/10.1016/j.actaastro.2016.05.007

World Resources Institute. *Forest Monitoring, Land Use & Deforestation Trends | Global Forest Watch*. https://www.globalforestwatch.org/

Wulder, M. A., Bater, C. W., Coops, N. C., Hilker, T., & White, J. C. (2008). The role of LiDAR in sustainable forest management. *The Forestry Chronicle*, *84*(6), 807–826. https://doi.org/10.5558/tfc84807-6

Xi, Z., Xu, H., Xing, Y., Gong, W., Chen, G., & Yang, S. (2022). Forest Canopy Height Mapping by Synergizing ICESat-2, Sentinel-1, Sentinel-2 and Topographic Information Based on Machine Learning Methods. *Remote Sensing*, *14*(2), Article 2. https://doi.org/10.3390/rs14020364

Xiang, W., Zhou, J., Ouyang, S., Zhang, S., Lei, P., Li, J., Deng, X., Fang, X., & Forrester, D. I. (2016). Species-specific and general allometric equations for estimating tree biomass components of subtropical forests in southern China. *European Journal of Forest Research*, *135*(5), 963–979. https://doi.org/10.1007/s10342-016-0987-2

Xiaoye Liu. (2008). Airborne LiDAR for DEM generation: Some critical issues. *Progress in Physical Geography: Earth and Environment*, *32*(1), 31–49. https://doi.org/10.1177/0309133308089496

Zimmerman, D., Pavlik, C., Ruggles, A., & Armstrong, M. P. (1999). An Experimental Comparison of Ordinary and Universal Kriging and Inverse Distance Weighting. *Mathematical Geology*, *31*(4), 375–390. https://doi.org/10.1023/A:1007586507433

Appendix A

Return #	Title	Year	Location	In-situ	RPAS	Aerial	Satellite	Interpolation	Satellite Resolution	Plot Areas	Number of Plots	Tree Carbon Estimation Method	Inclusion/Exclusion	Accuracy	Models used?
1	Comparison of methods toward multi-scale forest carbon mapping and spatial uncertainty analysis: combining national forest inventory plot data and landsat TM images	2015	Southern Illinois, USA	Forest inventory analysis (FIA)	N/A	N/A	Landsat TM	3 methods, regression, sequential gaussian co-simulation, and block co-simulation	30m	7.32 m radius, 24 ft, circular plots, lots of detail in the article	41 in 2004 and 38 in 2005	Once a species was assigned to each tree, total aboveground volume was estimated using species, measured DBH and height, and the FIA species-specific volume models (USDA FS 2009d). Biomass was then estimated using species group models (Jenkins et al. 2004), and finally, carbon content was estimated from biomass using the FIA conversion coefficient of 0.5 (Blackard et al. 2008; Dong et al. 2003; Gibbs et al. 2007; Peltoniemi et al. 2006; Tan et al. 2007).	"Using FIA methods, plot-level carbon stock for the additional plots was calculated as the sum of carbon estimates for all trees on plots, including the live trees that had the values of DBH \12.7 cm. However, standing dead trees with DBH \12.7 cm, samplings, and seedlings were excluded."	" The absolute percentage deviations of the predicted means from the observed average values were less than 36.8 % for the FIA plots and 35.1 % for the additional plots, respectively. "	Not Reported
2	Multi-scale Drivers of Spatial Variation in Old-Growth Forest Carbon Density Disentangled with Lidar and an Individual-Based Landscape Model	2012	"The HJ Andrews Experimental Forest (HJA) is located at N44.2, W122.2 in the western Cascade 1322 R. Seidl and others Range of Oregon."	"Forest inventory data Field data were assembled from a variety of previous vegetation-related projects at HJA (see Harmon and Munger 2005), and consequently were of different plot sizes and clustered over the landscape."	N/A	"airborne discrete return Lidar data (see Lefsky and others 2002) were collected on August 10 and 11, 2007 by Watershed Sciences, Inc. (Corvallis, Oregon, USA). Lidar was collected by a fixed wing aircraft equipped with a Leica ALS50 Phase II laser scanner with a 59 kHz pulse rate, scan angle of ±14, and scan swath overlap of at least 50%. Average Lidar point return density exceeded 9 m-2 within the study area, and root mean squared error between 344 real-time kinematic ground survey points and Lidar data was 0.024 m."	N/A	"spatially explicit information on vegetation structure and composition were derived from gradient nearest neighbor (GNN) imputation of forest inventory data (Ohmann and others 2011)."	N/A	Variable	41	" From field data on tree size and abundance per 25 m by 25 m plot aboveground live C (ALC) was derived by means of allometric equations. To increase the robustness of this ALC estimate, we used the average over two different sets of allometric equations (Means and others 1994; Jenkins and others 2004)."	Not Reported	the word accuracy was not used once in the manuscript and comparisons between forest inventory data and LiDAR or iLand were not given.	iLAND, individual based forest landscape and disturbance model
3	Multi-scale processes influencing global carbon storage and land-carbon-climate nexus: A critical review	2023	Global	N/A	N/A	N/A	N/A	N/A	N/A	Variable	N/A	Not Reported	Not Reported	Not Reported	Not Reported
4	Multi-scale controls of historical forest-fire regimes: new insights from fire-scar networks	2011	Western North America, including diverse forest types such as ponderosa pine (Pinus ponderosa) forests in the southwestern United States and mixed conifer forests in northern regions.	in-situ sampling of fire scars directly from trees at multiple sites to reconstruct historical fire events. Sampled trees include species known for their longevity and fire-scar preservation abilities	N/A	N/A	N/A	Interpolated to landscape scales, but did not mention a specific interpolation method.	N/A	Fire-scar networks cover hundreds to thousands of hectares at each site, with variability depending on the study region. Full inventory consisted of >100ha fire scar networks	Not Reported	N/A	Inclusion: Trees selected for fire-scar sampling must have visible, datable fire scars and belong to species with long-lived, fire-resistant traits. Exclusion: Trees without fire scars or those in forest areas lacking evidence of historical fires were excluded.	Not Reported	fire-scar network analysis models
5	The North American carbon program multi-scale synthesis and terrestrial model intercomparison project–Part 1: Overview and experimental design	2013	North America, FLUXNET Sites: The study incorporates data from FLUXNET tower networks across North America, providing ecosystem-level carbon flux measurement and Data from forest inventory plots across North America contribute to carbon stock estimates	in-situ observational data from various sources, including flux towers, forest inventories, and soil carbon measurements to validate and constrain model outputs.	N/A	N/A	MODIS, Landsat, AVHRR, GRACE, ASTER	Upscaling/Downscaling, specific interpolation methods aren't mentioned by it can be assumed to use IDW, krigging, or spline. Data from MODIS, etc are pre-interpolated	Ranges from 30m to 300km resolutions	Varying plots sizes	Not Reported	DBH Allometric equations	includes TBMs that simulate carbon dynamics across North America and have the capability to perform standardized simulations as per the project's experimental design	N/A	Biome-BGC, CLM4, DLEM, ISAM, LPJ-wsl, SiB3, SiBCASA, TEM6, VEGAS2.1, VISIT
6	A large-scale forest landscape model incorporating multi-scale processes and utilizing forest inventory data	2013	Missouri Ozarks in the United States,	Data from the U.S. Forest Service's Forest Inventory and Analysis (FIA) program	N/A	N/A	N/A	Not Reported	N/A	0.067 ha	1200	DBH allometric equations	FIA plots	Model accuracy is assessed by comparing simulated outputs with observed data, reporting a coefficient of determination (R^2) of 0.85,	LANDIS PRO
7	Community forest management and the emergence of multi-scale governance institutions: Lessons for REDD+ development from Mexico, Brazil and Bolivia	2011	Mexico, Brazil, and Bolivia, analyzing CFM systems within these countries.	in-situ observations and CFM analyses	N/A	N/A	N/A	N/A	N/A	Varying plots sizes	N/A	N/A	The research includes CFM systems that have developed multi-scale governance institutions, particularly those relevant to REDD+ development.	N/A	Case Studies
8	Detecting forest degradation in the three-north forest shelterbelt in China from multi-scale satellite images	2021	Three-North Forest Shelterbelt in China, encompassing the northeastern, northwestern, and northern regions of the country. 4.07 × 106 km2	ground survey data to validate the forest degradation maps derived from satellite imagery	N/A	N/A	MODIS/LandSAT	Temporal Interpolation	30, 250, 1000	Not Reported	N/A	N/A	The analysis includes areas within the Three-North Shelterbelt with available satellite data and excludes regions with insufficient data or cloud cover.	As High as 84.35%	
9	Multi-scale lidar measurements suggest miombo woodlands contain substantially more carbon than thought	2024	miombo woodlands in and around Gilé National Park, Mozambique, covering approximately 50,000 hectares.	The study includes terrestrial laser scanning (TLS) to capture detailed 3D measurements of individual trees, providing precise data on tree structure and biomass	UAV-LS covered six 300ha sections	Helicopor ALS covered entire area	GEDI, 18,611 footprints	Machine learning algorithms, specifically XGBoost, are employed to interpolate and predict aboveground biomass across the study area by integrating data from TLS, UAV, aerial, and satellite sources	25m diameter shits, 60m apart	TLS - 1 ha plots	6 TLS, 6 ALS, 18,611 GEDI plus varying plots from other sources	Allometric Equations predicted from two miombo woodland-specific and one widely-used pan-tropical allometric models, respectively	The study includes areas within the miombo woodlands that are accessible and suitable for lidar data collection, excluding regions with dense canopy cover that may impede lidar penetration or areas with significant human disturbance	Not specifically mentioned but explians that new models report more accurately with 51% to 118% more AGB and results are more accurate for larger trees compared to smaller individuals	The study utilizes the XGBoost machine learning algorithm to model and predict aboveground biomass across the study area
10	Multi-scale predictions of massive conifer mortality due to chronic temperature rise	2016	Southwestern United States	The research utilizes empirical data on predawn water potential thresholds for dominant NET species, determining the points at which photosynthesis, hydraulic and stomatal conductance, and carbohydrate availability approach zero	N/A	N/A	N/A	Regional models, type not specified	N/A	Regional,no specific plot size		N/A	NET Species		dynamic global vegetation models (DGVMs)
11	Estimating urban above ground biomass with multi-scale LiDAR	2018	London, UK	TLS, individual tree level, 10,000 ppsm	N/A	0.5m resolution, 4 ppsm of London Borough of Camden	N/A	N/A	N/A	N/A	TLS - 66 trees	Borough-wide allometry (chave et al) (using TLS to estimate AGB and derive allometry	Included: Trees that were mature, accessible, and adequately captured in TLS or airborne LiDAR datasets. Excluded: Trees with partial data (e.g., obstructed views, low point density)	ALS had a 20% RSME compared TLS	Regression
12	Multi-scale influence of vapor pressure deficit on fire ignition and spread in boreal forest ecosystems	2014	Interior Alaska for Boreal Forests	Alaska Lightning Detection Network (ALDN) data	N/A	N/A	MODIS active fire product, MODIS vegetation index	Aggregated/temporal most likely spline or IDW		Regional,no specific plot size	N/A	N/A	Included: All detected fire events within the study period (2002–2011) and region. Excluded: Areas outside interior Alaska and fire events without sufficient data.	The study found a significant relationship between daily VPD and the likelihood of lightning-induced fire ignition	Regression
13	Developing a forest data portal to support multi-scale decision making	2012	Global	Ground-based aboservatuons	Doesn't specify, but allows drone data integration	aerial photography and Lidar scans at various resolutions	Doesn't mention specific satellites but includes vegetation indexes and landcover classification	IDW and kriging to harmonize different datasets	varies	varies	N/A	Allometric Equations	Included: quality meeting data	N/A	Multiple
14	Evaluating forest transition based on a multi-scale approach: forest area dynamics in Switzerland 1850–2000	2016	Switzerland	Historical maps and national forest inventory data (ground surveys)	N/A	N/A	N/A	Not Mentioned	N/A	Not mentioned, but multiple	N/A	N/A, focuses on dynamics not carbon	Not Reported	inaccuracies exist due to differences in mapping techniques and inventory data	N/A
15	The potential of the Geostationary Carbon Cycle Observatory (GeoCarb) to provide multi-scale constraints on the carbon cycle in the Americas	2018	Americas, from North of Canada to south of South America	FLUXNET, NOAA's global monitoring network, TCCON	Not used, but was anticipated	NASA Carve, ACT-America,, Airborn LiDAR and hyperspecteral	OCO-2, TROPONI, MODIS, GEDI	Not Mentioned	varies,	N/A	N/A	N/A	N/A	Not Reported	Atmospheric Transport models, ecosystem models

Appendix A (Continued)

Return #	Title	Year	Location	In-situ	RPAS	Aerial	Satellite	Interpolation	Satellite Resolution	Plot Areas	Number of Plots	Tree Carbon Estimation Method	Inclusion/Exclusion	Accuracy	Models used?
16	Multi-scale estimation of the effects of pressures and drivers on mangrove forest loss globally	2020	Global mangrove forests	N/A	N/A	N/A	Global Mangrove Watch dataset and Global Forest Change dataset	Not Mentioned	25m-30m	N/A	N/A	Not Reported	included: mangroves indentified in 1996, 2007, and 2016	95% overall accruacy in mangrove extent classifcation	baysian heirarchical models
17	From sample to pixel: multi-scale remote sensing data for upscaling aboveground carbon data in heterogeneous landscapes	2018	Brazil	60 field plots, 1 ha size, DBH and tree height for >5cm dbh trees	N/A	N/A	RapidEye imagery, Hyperion Hyperspecteral imagery from EO-1	Cartographic method, surface method, regression	5m and 30m respectively	0.1	60	Local allometric equations	included: Field plots fully contained within a single Hyperion pixel to ensure accurate spatial correspondence.	Larger datasets has better AGC models	Random forest regression
18	Reviews and synthesis: Carbonyl sulfide as a multi-scale tracer for carbon and water cycles	2018	Global	Data from flux tower (eddy covariance)	N/A	N/A	Mentions but does not utilize	Not Mentioned	N/A	N/A	N/A	GPP	N/A	N/A	Atmospheric Transport models, ecosystem models
19	Spatially-explicit modeling of multi-scale drivers of aboveground forest biomass and water yield in watersheds of the Southeastern United States	2017	Southeasternn United States	N/A	N/A	N/A	Landcover data, Climate Data (PRISM Climate group), DEMS, Soil (SSURGO database)	GWR	N/A	N/A	N/A	Not mentioned but allometric equations	Included: Watersheds within the SE US with available data on climate, land cover, topography, and soil properties	Not Reported	WaSSI, GWR
20	A Multi-Scale Forest Above-Ground Biomass Mapping Approach: Employing a Step-by-Step Spatial Downscaling Method with Bias-Corrected Ensemble Machine Learning	2024	China, Daxing'anling Mountains and Xiaoxing'anling Mountains	N/A	N/A	N/A	Existing Global AGB datasets, LandSAT, MODIS, Terra, Aqua, Sentinel-2, SRTM,	Step by Step Downscaling	Varies, 30m+	N/A	N/A	Not Reported	Included: areas with available coase-resoluton AGB data	The combination of XGBoost for initial AGB mapping and Random Forest for residual correction yielded superior accuracy	XGBoost, Random Forest
21	Multi-scale integration of satellite remote sensing improves characterization of dry-season green-up in an Amazon tropical evergreen forest	2020	Brazil	pheocam observations (timelapse) to monitor canpy dynamics	N/A	N/A	PlaneScope, MODIS	Cross calibration, Linear specteral mixture analysis	3-500m	N/A	N/A	N/A	Areas that had both planetscope and MODIS coverage	Seasonal variations in GV and NPV fractions derived from PlanetScope closely matched ground-based phenocam observations, demonstrating strong agreement	Linear Specteral Mixture Models, BRDF adjustment models
22	Keeping pace with forestry: Multi-scale conservation in a changing production forest matrix	2020	Sweden	Forest-associated specie, conservation measures, and practices	N/A	N/A	N/A	N/A	N/A	N/A	N/A	N/A	N/A	N/A	N/A
23	Accounting for carbon and nitrogen interactions in the global terrestrial ecosystem model ORCHIDEE (trunk version, rev 4999): multi-scale evaluation of gross primary production	2019	Global	78 FLUXNET sites, 0.1 to 1 km2	N/A	N/A	MODIS LAI	Not Mentioned	1km2	0.1 to 1km2	78	GPP	N/A	N/A	ORCHIDEE
24	All-carbon multi-scale and hierarchical fibers and related structural composites: A review	2020	N/A	N/A	N/A	N/A	N/A	N/A	N/A	N/A	N/A	N/A	N/A	N/A	N/A
25	Estimating vegetation primary production in the Heihe River Basin of China with multi-source and multi-scale data	2016	China, Heihe River Basin	Ground measurements at flux towers for GPP, 0.1 to 1km2	N/A	N/A	HiWATER, USGS HYDRO1k, GLDAS	N/A	Varies	0.1 to 1km2	N/A	GPP, NPP	N/A	RMSE of 2.973 gC m^{-2} d^{-1} and a R of 0.842 when compared with ground-based GPP measurements	MuSyQ-NPP
26	Multi-scale assessment of forest cover in an agricultural landscape of Southeastern Brazil: Implications for management and conservation of stream habitat and water quality	2018	Southeastern Brazil	Field assessments to analyze streams, 18 catchments (2nd -4th order streams)	N/A	N/A	Not mentioned, Landcover products	N/A	N/A	2nd - 4th order catchments	68	N/A	N/A	N/A	simple and multiple linear regression
27	Multi-scale validation of GLEAM evapotranspiration products over China via ChinaFLUX ET measurements	2017	China	Fluxtowers from ChinaFLUX 0.1 to 1km2	N/A	N/A	GLEAM ET	N/A	25km2	0.1 to 1km2	N/A	N/A	N/A	R = 0.71 to 0.86 depending on temporal aspect	GLEAM
28	Prediction of mechanical properties of carbon nanotube-carbon fiber reinforced hybrid composites using multi-scale finite element modelling	2019	N/A	N/A	N/A	N/A	N/A	N/A	N/A	N/A	N/A	N/A	N/A	N/A	N/A
29	Mapping spatial distribution of larch plantations from multi-seasonal Landsat-8 OLI imagery and multi-scale textures using random forests	2015	Northern China	Data collected to validate reults, plot numbers not specified	N/A	N/A	Landsat-8 OLI covering 90,000 ha		30m	N/A	N/A	N/A	N/A	The Random Forest classifier achieved an overall accuracy of 92.7% for identifying larch plantations, with a Kappa coefficient of 0.834.	Random forest regression, Texture Analysis
30	Multi-scale sensitivity of Landsat and MODIS to forest disturbance associated with tropical cyclones	2014	Temperate and Tropical rain forests (Australia, US)	0.1 to 1 ha plots used to collect DBH, height, species, mortality rates,	N/A	N/A	Landsat, MODIS	N/A	30m	N/A	N/A	N/A	Areas affected by Cyclones were included in the study	Landsat data effectively detected forest disturbances at the local scale, capturing variations within and between forest types. MODIS data accurately represented disturbance patterns at landscape and regional scales, including topographic effects and wind direction influences.	Specteral Mixture Analysis
31	Smoldering combustion and ground fires: ecological effects and multi-scale significance	2013	N/A	N/A	N/A	N/A	N/A	N/A	N/A	N/A	N/A	N/A	N/A	N/A	N/A
32	Evaluating MODIS-vegetation continuous field products to assess tree cover change and forest fragmentation in India – A multi-scale satellite remote sensing approach	2017	India	Ground truth data for validating, no plot size or number specified		N/A	MODIS	N/A	250m	N/A	N/A	N/A	Areas in India with varying degrees of forest cover and fragmentation	N/A	Remote Sensing Analysis
33	Biodiversity consequences of land-use change and forest disturbance in the Amazon: A multi-scale assessment using ant communities	2016	N/A	N/A	N/A	N/A	N/A	N/A	N/A	N/A	N/A	N/A	N/A	N/A	N/A
34	Multi-scale remote sensing-assisted forest inventory: A glimpse of the state-of-the-art and future prospects	2019	N/A	N/A	N/A	N/A	N/A	N/A	N/A	N/A	N/A	N/A	N/A	N/A	N/A
35	Impact assessment of the EU import ban on Indonesian palm oil: Using environmental extended multi-scale MRIO	2022	N/A	N/A	N/A	N/A	N/A	N/A	N/A	N/A	N/A	N/A	N/A	N/A	N/A

Appendix A (Continued)

Return #	Title	Year	Location	In-situ	RPAS	Aerial	Satellite	Interpolation	Satellite Resolution	Plot Areas	Number of Plots	Tree Carbon Estimation Method	Inclusion/Exclusion	Accuracy	Models used?
36	The North American carbon program multi-scale synthesis and terrestrial model intercomparison project–Part 2: Environmental driver data	2014	N/A	N/A	N/A	N/A	N/A	N/A	N/A	N/A	N/A	N/A	N/A	N/A	N/A
37	A multi-scale analysis of western spruce budworm outbreak dynamics	2017	BC, Canada	N/A	N/A	Aerial Survey was used across the study period	Landsat	Spatial Interpolation	30m	N/A	N/A	N/A	Included: Areas within British Columbia with documented western spruce budworm activity. Excluded: Regions without significant budworm presence or lacking sufficient data.	The study evaluates the accuracy of outbreak mapping by comparing aerial survey data with satellite imagery, though specific accuracy metrics are not detailed.	Analytical models
38	Multi-scale mechanical improvement produced in carbon nanotube fibers by irradiation cross-linking	2013	N/A	N/A	N/A	N/A	N/A	N/A	N/A	N/A	N/A	N/A	N/A	N/A	N/A
39	Spatial patterns of logging-related disturbance events: a multi-scale analysis on forest management units located in the Brazilian Amazon	2020	N/A	N/A	N/A	N/A	N/A	N/A	N/A	N/A	N/A	N/A	N/A	N/A	N/A
40	Multi-scale interlaminar fracture mechanisms in woven composite laminates reinforced with aligned carbon nanotubes	2014	N/A	N/A	N/A	N/A	N/A	N/A	N/A	N/A	N/A	N/A	N/A	N/A	N/A
41	Exploring the synergistic use of multi-scale image object metrics for land-use/land-cover mapping using an object-based approach	2015	China	N/A	N/A	N/A	SPOT-5	N/A	10m and 2.5m	N/A	84 sample sites for images	N/A	Included: Various land-use and land-cover types present within the study area.	"overall accuracy was 88.58% and had a κ value of 0.8560 in the classification using multi-scale object metrics. The detection of Moso bamboo forest was satisfactory, with a producer's accuracy of 96.60% and user's accuracy of 88.64%. High accuracy was also observed for broadleaf forest, yielding producer's and user's accuracies of 93.10% and 99.08%, respectively. A high rate of error occurred, with incorrect assignments occurring for a proportion of infrastructure to farmland assessments, which resulted in a relatively low user's accuracy for this category.	a object-based image analysis (OBIA) framework was employed, utilizing multi-scale segmentation and classification algorithms to map LULC types
42	Multi-scale heterogeneity in vegetation and soil carbon in exurban residential land of southeastern Michigan, USA	2016	Michigan, USA	Field measurements were conducted for vegetation and soil carbon storage, 26 total plots that were regionally representative	N/A	Aerial photointerpretation was conducted to identify land cover types and scale c storage to neighbourhoods	N/A	not mentioned	N/A	N/A	66	DBH Allometric equations	Included: Various ecological zones within residential parcels, such as turfgrass areas, dense woody vegetation, and impervious surfaces.	Not mentioned	Allometric equations
43	Beyond the'local community': the evolution of multi-scale politics in Nepal's community forestry regimes	2014	Nepal	N/A	N/A	N/A	N/A	N/A	N/A	N/A	N/A	N/A	N/A	N/A	N/A
44	Tropical forest disaster monitoring with multi-scale sensors from terrestrial laser, UAV, to satellite radar	2017	Robson Creek tropical forest, Australia	TLS data at 0.5m resolution to validate tree height in UAV data	DJI Phanton 3 (UAV-SfM)	2014 scans used, 10 points per 5x5m for tree heights	PALSAR 2, ALOS-2		3.125m	25 ha plots gridded over the research area subdivided into 1ha plot	25	Identifies forest gaps not biomass	Included: Areas within the tropical forest where disturbances or gaps were detectable using the employed remote sensing technologies.	The study emphasizes the importance of comparing UAV-derived DSMs with satellite radar data to understand backscatter characteristics, though specific accuracy metrics are not detailed in the available summary.	N/A
45	Multi-scale hybrid composites-based carbon nanotubes	2011	N/A	N/A	N/A	N/A	N/A	N/A	N/A	N/A	N/A	N/A	N/A	N/A	N/A
46	A multi-sensor, multi-scale approach to mapping tree mortality in woodland ecosystems	2020	Pihon-juniper lands in San Juan County, Utah, USA		Collected using a DJI Phanton 3, flying 100m AGL (83.6 ha) image data was collected to create georeferenced orthomosaics	LiDAR data collected using a Optech Titan esnor, flying height of 600m AGL at a speed of 82m/s at a pulse density of 21.3/m2	LandSat 8 acquired	N/A	30m	N/A	N/A	Does not look at tree carbon. The methodology combines UAS imagery for detailed, individual tree mortality assessment, airborne LiDAR for canopy structure analysis, and Landsat imagery for regional scaling.	N/A	The study reports that 39% of the PJ woodlands experienced some level of mortality, with patches exceeding 50% mortality. However, specific accuracy metrics for the mapping approach are not detailed in the available summary. "Although no formal accuracy assessment of our tree crown delineation algorithm was performed, a qualitative, visual assessment reveals that crowns shapes and sizes were accurately represented, though there were certainly examples of under- and over-segmentation"	N/A
47	Multi-scale toughening of fibre composites using carbon nanofibres and z-pins	2016	N/A	N/A	N/A	N/A	N/A	N/A	N/A	N/A	N/A	N/A	N/A	N/A	N/A
48	Testing a multi-scale scenario approach for smallholder tree plantations in Indonesia and Vietnam	2013	N/A	N/A	N/A	N/A	N/A	N/A	N/A	N/A	N/A	N/A	N/A	N/A	N/A
49	Predicting China's carbon price based on a multi-scale integrated model	2022	N/A	N/A	N/A	N/A	N/A	N/A	N/A	N/A	N/A	N/A	N/A	N/A	N/A
50	A multi-scale approach to detecting standing dead trees in UAV RGB images based on improved faster R-CNN	2023	Changsha County, Changsha City, Hunan Province in the People's Republic of China	N/A	DJI Matrice M300 RRTK with a DJI Zenmuse H20T. Flight speed of 8m/s at 150m AGL with frontal overlap of 75% and side overlap of 70% to create orthomosaic	N/A	N/A	Bilinear interpolation	N/A	N/A	4	Tests tree mortality not tree carbon	The proposed algorithm achieved an accuracy of 95.9% in identifying SDTs within UAV RGB images, indicating high reliability in detection performance.		
51	A multi-scale approach to coping with climate change and other collective action problems	2011	N/A	N/A	N/A	N/A	N/A	N/A	N/A	N/A	N/A	N/A	N/A	N/A	N/A
52	Multi-scale relationship between peatland vegetation type and dissolved organic carbon concentration	2012	Bingley Moor, Yorkshire, northern England (53-52' N, 1-8° W), and drain-scale analysis conducted at 32 blanket bog sites across England and Scotland	Dissolved organic carbon (DOC) data collected from plot-scale pore waters and surface water from artificial drains	N/A	N/A		N/A	n/a	Plot-scale study at Bingley Moor with approximately 1 meter depth peatlands; national survey drain sites typically <0.1 km².	n/a (stidy focuses on vegetation types within peatlands)	n/a	n/a		Statistical models, including one-way ANOVA and Bonferroni multiple-comparison tests for DOC concentrations
53	Multi-scale dynamics and environmental controls on net ecosystem CO2 exchange over a temperate semiarid shrubland	2018	Yanchi Research Station, Ningxia, North China (37°42'31"N, 107°13'37"E, 1530m a.s.l.)		N/A	N/A	N/A	N/A	N/A	N/A	N/A	N/A	N/A	N/A	N/A
54	Invasive alien plants as an alternative resource for concrete production – multi-scale optimization including carbon compensation, cleared land and saved water runoff in South Africa	2021	South Africa	Included	N/A	N/A	N/A	N/A	N/A	N/A	N/A	N/A	N/A	N/A	N/A
55	Multi-sensor, multi-scale, Bayesian data synthesis for mapping within-year wildfire progression	2019	Elephant hill, north of Ashcroft, British Columbia	Included	N/A	N/A	Landsat-8, Sentinel-2, and MODIS	N/A	500m	N/A	N/A	N/A	N/A	N/A	N/A